

# Tissue memory B cell repertoire analysis after ALVAC/AIDSVAX B/E gp120 immunization of rhesus macaques

Kan Luo,<sup>1</sup> Hua-Xin Liao,<sup>1,2,3</sup> Ruijun Zhang,<sup>1</sup> David Easterhoff,<sup>1</sup> Kevin Wiehe,<sup>1</sup> Thaddeus C. Gurley,<sup>1</sup> Lawrence C. Armand,<sup>1</sup> Ashley A. Allen,<sup>1</sup> Tarra A. Von Holle,<sup>1</sup> Dawn J. Marshall,<sup>1</sup> John F. Whitesides,<sup>1</sup> Jamie Pritchett,<sup>1</sup> Andrew Foulger,<sup>1</sup> Giovanna Hernandez,<sup>1</sup> Robert Parks,<sup>1</sup> Krissey E. Lloyd,<sup>1</sup> Christina Stolarchuk,<sup>1</sup> Sheetal Sawant,<sup>1</sup> Jessica Peel,<sup>1</sup> Nicole L. Yates,<sup>1</sup> Erika Dunford,<sup>1</sup> Sabrina Arora,<sup>1</sup> Amy Wang,<sup>1</sup> Cindy M. Bowman,<sup>1</sup> Laura L. Sutherland,<sup>1</sup> Richard M. Scearce,<sup>1</sup> Shi-Mao Xia,<sup>1</sup> Mattia Bonsignori,<sup>1,2</sup> Justin Pollara,<sup>4</sup> R. Whitney Edwards,<sup>4</sup> Sampa Santra,<sup>5</sup> Norman L. Letvin,<sup>5</sup> James Tartaglia,<sup>6</sup> Donald Francis,<sup>7</sup> Faruk Sinangil,<sup>7</sup> Carter Lee,<sup>7</sup> Jaranit Kaewkungwal,<sup>8</sup> Sorachai Nitayaphan,<sup>9</sup> Punnee Pitisuttithum,<sup>10</sup> Supachai Reks-ngarm,<sup>11</sup> Nelson L. Michael,<sup>12</sup> Jerome H. Kim,<sup>12</sup> S. Munir Alam,<sup>1,2,13</sup> Nathan A. Vandergrift,<sup>1,2</sup> Guido Ferrari,<sup>1,4</sup> David C. Montefiori,<sup>4</sup> Georgia D. Tomaras,<sup>1,4,14</sup> Barton F. Haynes,<sup>1,2,14</sup> and M. Anthony Moody<sup>1,14,15</sup>

<sup>1</sup>Duke Human Vaccine Institute, <sup>2</sup>Department of Medicine, Duke University Medical Center, Durham, North Carolina, USA. <sup>3</sup>College of Life Science and Technology, Jinan University, Guangzhou, China. <sup>4</sup>Department of Surgery, Duke University Medical Center, Durham, North Carolina, USA. <sup>5</sup>Center for Virology and Vaccine Research, Beth Israel Deaconess Medical Center, Harvard Medical School, Boston, Massachusetts, USA. <sup>6</sup>Sanofi-Pasteur, Swiftwater, Pennsylvania, USA. <sup>7</sup>Global Solutions for Infectious Diseases, South San Francisco, California, USA. <sup>8</sup>Center of Excellence for Biomedical and Public Health Informatics BIOPHICS, Faculty of Tropical Medicine, Mahidol University, Bangkok, Thailand. <sup>9</sup>Armed Forces Research Institute of Medical Sciences-Royal Thai Army Component, Bangkok, Thailand. <sup>10</sup>Mahidol University, Bangkok, Thailand. <sup>11</sup>Department of Disease Control, Ministry of Public Health, Nonthaburi, Thailand. <sup>12</sup>U.S. Military HIV Research Program, Walter Reed Army Institute of Research, Silver Spring, Maryland, USA. <sup>13</sup>Department of Pathology, <sup>14</sup>Department of Immunology, <sup>15</sup>Department of Pediatrics, Duke University Medical Center, Durham, North Carolina, USA.

The ALVAC prime/ALVAC + AIDSVAX B/E boost RV144 vaccine trial induced an estimated 31% efficacy in a low-risk cohort where HIV-1 exposures were likely at mucosal surfaces. An immune correlates study demonstrated that antibodies targeting the V2 region and in a secondary analysis antibody-dependent cellular cytotoxicity (ADCC), in the presence of low envelope-specific (Env-specific) IgA, correlated with decreased risk of infection. Thus, understanding the B cell repertoires induced by this vaccine in systemic and mucosal compartments are key to understanding the potential protective mechanisms of this vaccine regimen. We immunized rhesus macaques with the ALVAC/AIDSVAX B/E gp120 vaccine regimen given in RV144, and then gave a boost 6 months later, after which the animals were necropsied. We isolated systemic and intestinal vaccine Env-specific memory B cells. Whereas Env-specific B cell clonal lineages were shared between spleen, draining inguinal, anterior pelvic, posterior pelvic, and periaortic lymph nodes, members of Env-specific B cell clonal lineages were absent in the terminal ileum. Env-specific antibodies were detectable in rectal fluids, suggesting that IgG antibodies present at mucosal sites were likely systemically produced and transported to intestinal mucosal sites.

**Authorship note:** N.L. Letvin is deceased. K. Luo and H.X. Liao contributed equally to this work.

**Conflict of interest:** J. Tartaglia was an employee of Sanofi and D. Francis, F. Sinangil, and C. Lee were employees of Global Solutions for Infectious Diseases at the time this study was performed. D. Francis, F. Sinangil, and C. Lee are former employees of VaxGen.

**Submitted:** May 12, 2016

**Accepted:** November 1, 2016

**Published:** December 8, 2016

**Reference information:**

*JCI Insight.* 2016;1(20):e88522.  
doi:10.1172/jci.insight.88522.

## Introduction

The RV144 trial demonstrated 60% efficacy against infection at 6 months (1) and 31% efficacy at 2 years (2). An immune correlates analysis showed that decreased transmission risk correlated with high levels of plasma envelope-binding (Env-binding) antibodies against gp120 variable regions 1 and 2 (V1V2) (3). Antibody-dependent cellular cytotoxicity–mediating (ADCC–mediating) antibody levels and tier 1 neutralizing antibodies directly correlated with decreased transmission risk in the presence of low Env IgA antibodies (3). The IgA correlate of risk may have been due to specific Env-binding IgA antibodies

blocking the activity of ADCC antibodies (4). Moreover, plasma antibody binding to linear V2 and variable region 3 (V3) (5) as well as binding to V1V2 scaffold proteins from multiple HIV-1 isolates (6) also correlated with decreased infection risk. Higher IgG3 antibody responses against V1V2 have been suggested to be a primary effector IgG subclass (7–9). Sequencing of the transmitted/founder viruses isolated from RV144 vaccinees that did become infected demonstrated the lysine at position 169 (K169) in the V2 region as a site of selection pressure (10). Analyses of mAbs representative of the putative protective antibodies from RV144 subjects showed that the V2 K169–centered epitope is recognized by antibodies with restricted variable heavy ( $V_H$ ) and variable light ( $V_L$ ) chain gene usage (11) and that  $V_L$  restriction for recognition of the V2 epitope around K169 is conserved throughout primate phylogeny (12). Thus, the current hypothesis is that ADCC or other Fc receptor–mediated (FcR-mediated) anti-HIV-1 functions of V2 and other Env antibodies were the likely correlates of protection (7, 13–16).

The RV144 study did not include mucosal sampling, and therefore it has not been possible to test for the presence of antibodies at mucosal sites in vaccine recipients. Invasive sampling methods to obtain lymph nodes (LNs) or spleen tissues from vaccinees that can provide mechanistic insights into vaccine responses are logistically difficult or impossible in human populations. In order to perform a more detailed analysis of the antibody response to the RV144 vaccine, we undertook a study in rhesus macaques using the same vaccine regimen as that given to humans in RV144, performed LN and spleen sampling following the final immunization, and performed a memory B cell repertoire analysis to determine the specificity and location of RV144 vaccine-induced Env-reactive B cells.

## Results

*Epitope mapping of plasma antibody responses to RV144 vaccine Envs.* Five rhesus macaques (RMs) were immunized with the vaccine regimen used in RV144 (Figure 1A). The immunogens were ALVAC-HIV (vCP1521), a recombinant canarypox expressing HIV-1 Gag and Pro from B.LAI and HIV-1 gp120 from CRF01\_AE (92TH023) linked to the transmembrane anchoring portion of gp41 from B.LAI; and AIDS-VAX B/E, an alum-adjuvanted bivalent HIV-1 gp120 Env glycoprotein vaccine from strains E.A244 (E.CM244) and B.MN produced in Chinese hamster ovary cell lines. After receiving 2 immunizations of ALVAC-HIV alone, followed by 2 boosts with ALVAC-HIV with AIDS-VAX B/E, the animals were subsequently boosted with ALVAC-HIV and AIDS-VAX B/E at week 53, and 2 weeks later the animals were necropsied with extensive tissue sampling. Binding antigen multiplex assay (BAMA) (6) of the plasma demonstrated systemic antibody responses to the 3 Env isolates in the vaccine in all animals (Figure 1, G–I) as well as to the gp70 Case A2 V1V2 and C.1086 V1V2 tag proteins used in the RV144 correlates studies (Figure 1, J and K) (3, 6). We also observed binding to a scaffolded version of the V1V2 loop of AE.A244 (Figure 1L). For all animals, high titers of antibodies were detected after the fourth immunization as well as after the final boost.

We tested for the ability of plasma antibody to block the binding to gp120 of key V2 (CH58, CH59, CH01) and C1 (A32) targeted mAbs, and soluble CD4 (sCD4; Figure 1, B–F). As was observed in RV144 trial participants (17), at the end of the first 4 immunizations all animals developed high levels of mAb A32–blocking antibodies (Figure 1B). In addition, we observed blocking of sCD4 (Figure 1C). We also observed blocking of V2 mAbs CH58 and CH59 (Figure 1, D and E) and low-level blocking of the V2V3 broad neutralizing antibody (bnAb) CH01 (18) (Figure 1F).

*Functional activity of serum antibody responses to RV144 vaccine Envs.* TZM-bl neutralization assays of serum demonstrated that all animals had neutralization activity against the clade B strain in the vaccine (B.MN.3, Figure 2B) and 4 of 5 animals had activity against the clade CRF01\_AE strain in the ALVAC prime (AE.92TH023.6, Figure 2A). All animals had activity against heterologous isolates from clade B (B.SF162.LS, Figure 2C) and clade C (C.MW695.26, Figure 2E); 4 of 5 animals also developed activity against B.BaL.26 (Figure 2D). All animals had a decrease in neutralization activity immediately prior to the final boost and this activity was boosted against all tested strains except for animal 33-11 that did not boost neutralization against AE.92TH023.6 or B.BaL.26. These neutralization results are similar to those observed in serum from vaccinees in the RV144 trial (19).

We tested for ADCC activity mediated by plasma antibodies against target cells coated with gp120s reflective of 3 virus strains in the vaccine. The animals had little or no activity detectable in the prebleed samples, and all animals had activity detected in samples taken 2 weeks after the fourth immunization (Figure 2, F–N). Titration of plasma antibodies indicated high levels against all 3 strains (Figure 2, F–H), while

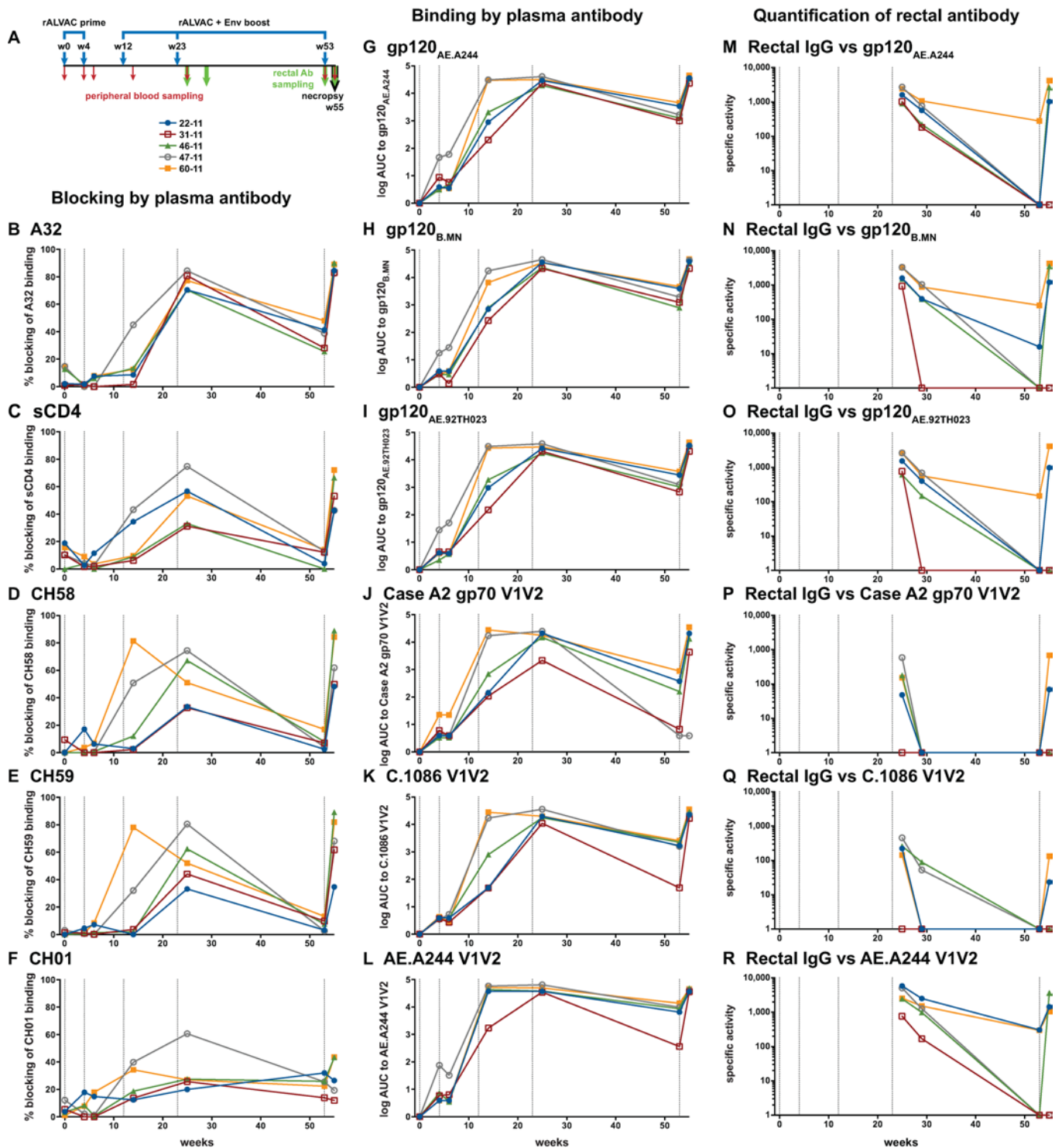


**Figure 1. Study schedule and antibody binding data.** (A) Five rhesus macaques (RMs) were immunized 5 times (blue arrows above timeline) and peripheral blood taken 7 times (red arrows), rectal antibody sampled 4 times (green arrows), and the animals necropsied 2 weeks after the final immunization (black arrow). Individual macaques are represented by the same symbols in all figures. In plots B–R, dotted vertical lines represent immunization time points. Plasma antibodies were tested for their ability to bind gp120<sub>AE.A244</sub> in ELISA and block the binding of mAb A32 (B), soluble CD4 (sCD4) (C), mAb CH58 (D), mAb CH59 (E), and bnAb CH01 (F). Plasma antibody binding in ELISA (plotted as log<sub>10</sub> AUC) was measured for gp120<sub>AE.A244</sub> (G), gp120<sub>B,MN</sub> (H), gp120<sub>AE.92TH023</sub> (I), Case A2 gp70 V1V2 (J), C.1086 V1V2 tags (K), and AE.A244 V1V2 tags (L). Rectal antibody was sampled using a surgical sponge inserted into the rectum and then eluted. Binding was measured and specific activity was calculated as specific activity = (antibody binding units × dilution factor)/measured rectal IgG in μg/ml for binding to gp120<sub>AE.A244</sub> (M), gp120<sub>B,MN</sub> (N), gp120<sub>AE.92TH023</sub> (O), Case A2 gp70 V1V2 (P), C.1086 V1V2 tags (Q), and AE.A244 V1V2 tags (R). RMs 22-11, 46-11, and 60-11 boosted rectal antibody with the final immunization; those animals were selected for B cell repertoire analysis.

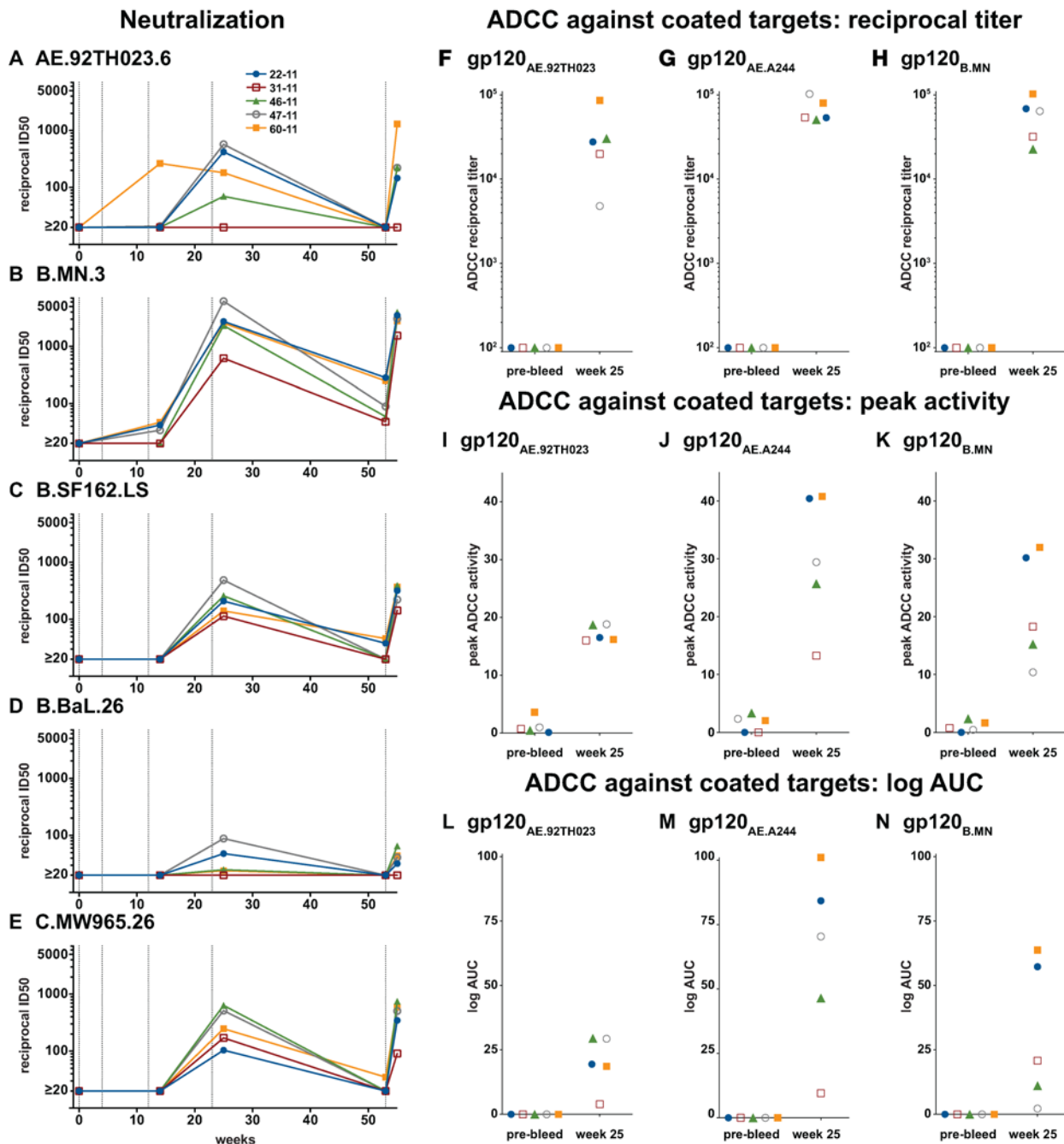


**Figure 2. Functional activity of plasma/serum antibody.** Serum antibody neutralization in the TZM-bl assay was measured for pseudoviruses AE.92TH023.6 (A), B.MN.3 (B), B.SF162.LS (C), B.BaL.26 (D), and C.MW965.26 (E). Plasma antibody-dependent cellular cytotoxicity (ADCC) activity was measured against gp120-coated targets for the AE.92TH023 (F, I, and L), AE.A244 (G, J, and M), and B.MN (H, K, and N). ADCC activity is shown as reciprocal ADCC titer (F–H), peak activity in the assay (I–K), and log AUC (L–N). All animals had a rise in functional antibodies following vaccination. ID50, inhibitory dilution 50%.

determination of peak activity showed variation among the 3 strains (Figure 2, I–K). Calculation of the area under the curve for the titration showed that activity was highest against the AE.A244 strain (Figure 2M), except for RM 31-11, which had higher activity against B.MN (Figure 2N). These results are similar to those observed for human participants in the RV144 trial (17).

*Detection of mucosal antibodies in immunized RMs.* Using surgical sponges, we sampled antibody present in the rectal mucosa at weeks 25 and 29, after the fourth immunization, and again at weeks 53 and 55, at the time of the final immunization and necropsy. The concentration of recovered IgG for each sample is shown in Supplemental Table 1; supplemental material available online with this article; doi:10.1172/jci.insight.88522DS1;

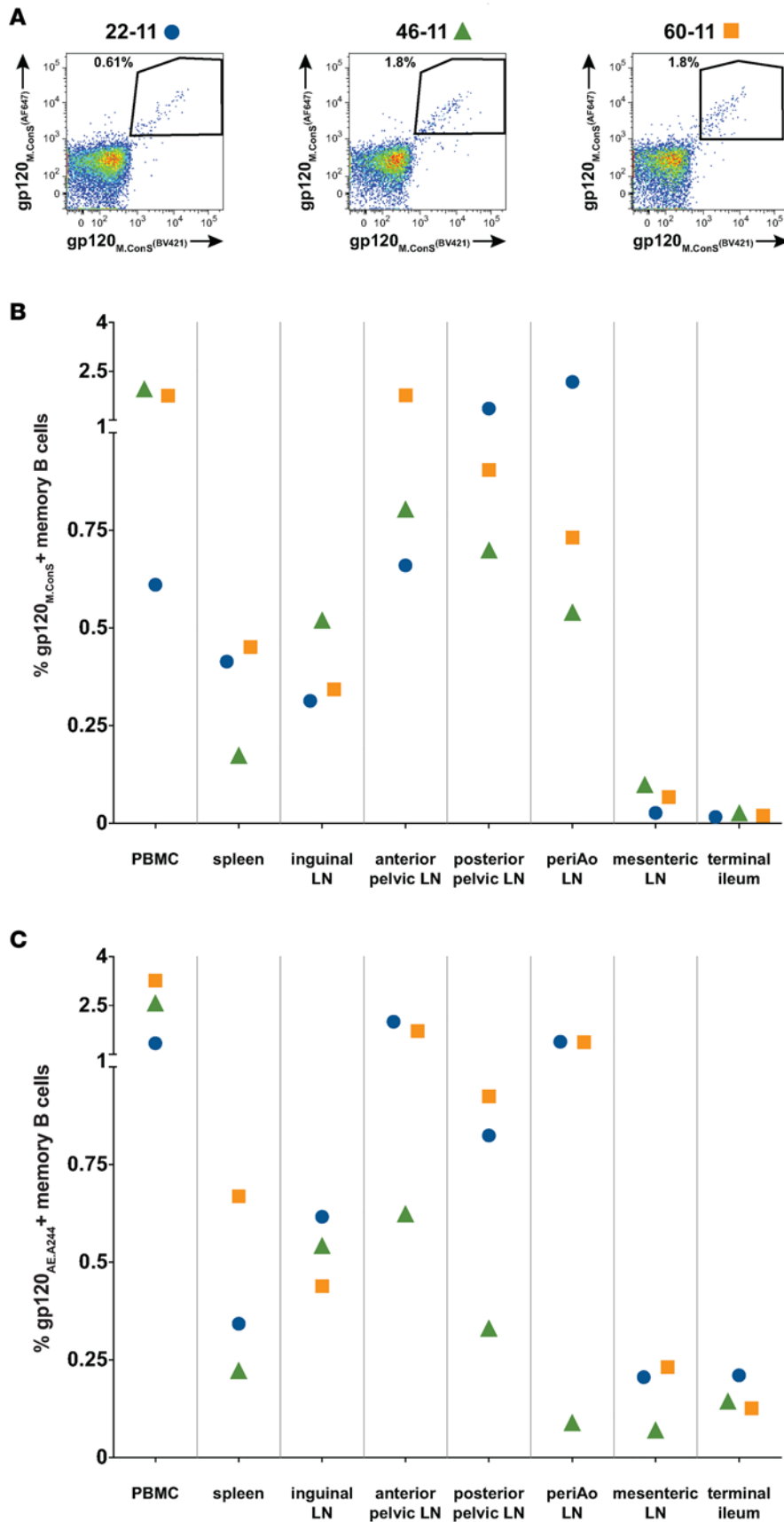


**Figure 3. Flow cytometric detection of antigen-specific B cells.** Peripheral blood mononuclear cells (PBMCs) were labeled to identify memory B cells, defined as CD3/14/16<sup>-</sup>, CD20<sup>+</sup>, and surface IgD<sup>-</sup>, and also with Env probes in 2 colors. **(A)** PBMCs labeled with gp120<sub>M,ConS</sub> in 2 colors are shown for the 3 rhesus macaques (RMs). **(B)** Cell samples from all sites obtained at necropsy were labeled with gp120<sub>M,ConS</sub> and shown as the frequency of memory B cells. Few antigen-specific B cells were observed in mesenteric lymph nodes (LNs) or terminal ileum. **(C)** Cell samples were also labeled with gp120<sub>AE,A244</sub> and showed a similar pattern, except that the detected cell frequency was lower for RM 46-11 (green triangles) in anterior pelvic LN, posterior pelvic LN, and periaortic LN. In mesenteric LN and terminal ileum, antigen-specific B cell frequencies were slightly higher for gp120<sub>AE,A244</sub> than they were for gp120<sub>M,ConS</sub>.

we recovered more than 0.085 µg/ml of IgG from all but 3 samples. Although there was not gross blood contamination of the specimens, we cannot rule out that blood may have contributed to detected antibody levels. After the fourth immunization, all animals had detectable IgG against gp120s reflective of the vaccine strains (Figure 1, M–O) and AE.A244 V1V2 (Figure 1R). When we assayed for binding to Case A2 gp70 V1V2 and C.1086 V1V2 scaffolded protein, we found that 4 of 5 RMs had detectable rectal antibody, but that RM 31-11 did not (Figure 1, P and Q). Detectable antibodies declined for all antigens after a 6-month rest, falling below the limit of detection for most animals, despite all but 1 animal (RM 46-11) having an IgG concentration above the limit of detection. After the final boost, 3 animals with sufficient recovery of rectal IgG (RMs 22-11, 46-11, and 60-11) were found to have substantial boosting of rectal antibody (Figure 1, M–R). In contrast with rectal antibody, plasma levels did not decline as substantially (Figure 1, G–L), raising the hypothesis that local production of antibody may have produced at least some of the antibodies detected in rectal fluid.

*Flow cytometric assessment of antigen-specific B cells from LN and spleen.* To assess whether anatomic distribution of B cells was responsible for the differences observed between plasma and rectal fluid, we performed antigen-specific B cell sorting of tissues. RMs 22-11, 46-11, and 60-11 were selected for further study because these animals had boosted mucosal antibodies following the final immunization (Figure 1,

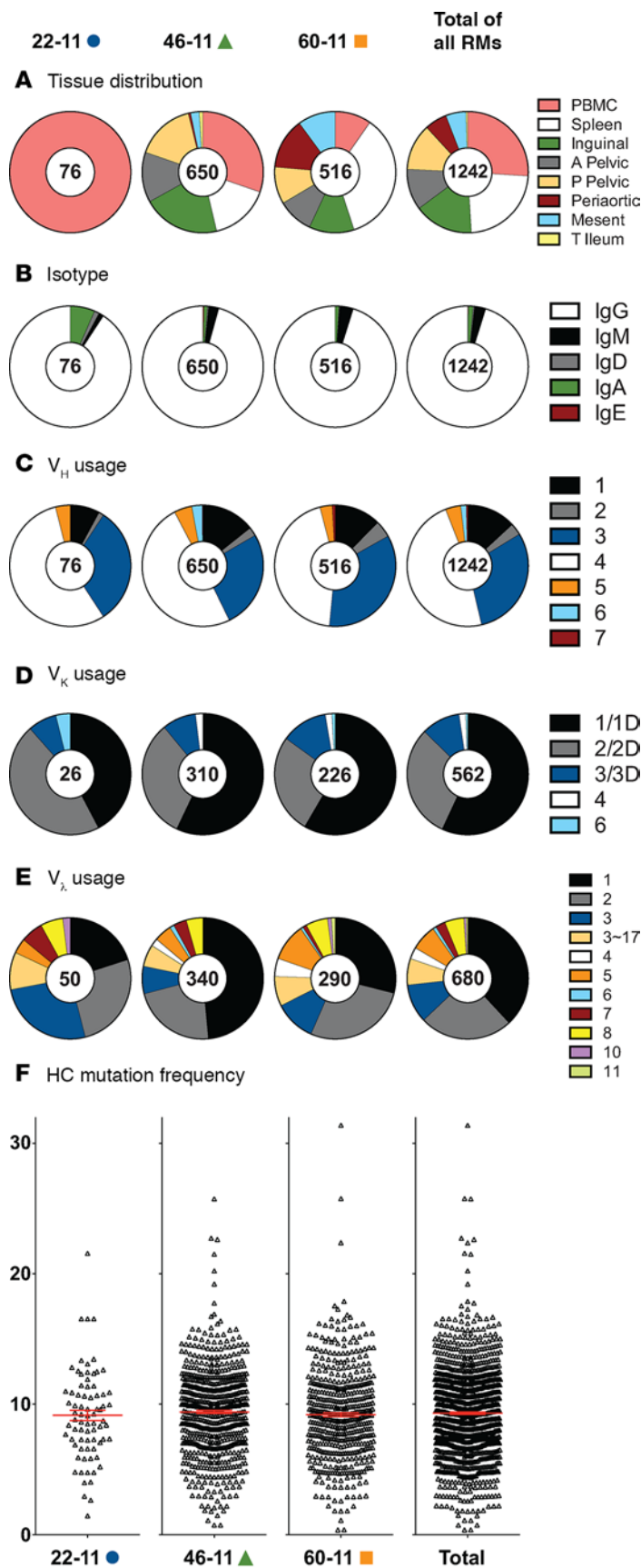


**Figure 4. Characteristics of isolated HIV-1 envelope-reactive mAbs.**

There were 1,493 mAbs isolated of which 1,242 were reactive with HIV-1 antigens during screening. (A) For rhesus macaque (RM) 22-11, mAbs were isolated only from peripheral blood mononuclear cells (PBMCs). For RMs 66-11 and 60-11, envelope-reactive (Env-reactive) mAbs were isolated from most tissue compartments. (B) The majority (95%) of isolated mAbs were of IgG isotype. (C) V<sub>H</sub> gene segment usage was similar among the RMs with the majority of mAbs using V<sub>H</sub>1, V<sub>H</sub>3, and V<sub>H</sub>4. Overall, 55% of mAbs used lambda chains. For kappa chain-using mAbs, the majority used V<sub>K</sub>1/1D or V<sub>K</sub>2/2D (D); for lambda chain-using mAbs, the majority used V<sub>λ</sub>1, V<sub>λ</sub>2, or V<sub>λ</sub>3 (E). Each animal had some Env-reactive mAbs that used V<sub>λ</sub>3~17, the lambda chain associated with genetically conserved V1V2 responses. (F) Heavy chain (HC) mutation frequencies were similar among Env-reactive antibodies for all 3 RMs; the overall mean mutation frequency was 9.3%.

M-R). At the week 55 necropsy, samples of peripheral blood mononuclear cells (PBMCs), spleen, inguinal LN, anterior pelvic LN, posterior pelvic LN, periaortic LN, mesenteric LN, and terminal ileum were taken and studied. Samples from each tissue were sorted using gp120<sub>M,Cons</sub>, gp120<sub>AE.A244</sub>, and AE.A244 V1V2 tags (11) as previously described (17); Supplemental Table 2 shows the number of memory B cells that were analyzed for each sorted tissue and Figure 3A shows examples of the observed patterns for gp120<sub>M,Cons</sub> binding to memory B cells, defined as CD3/14/16<sup>-</sup>, CD20<sup>+</sup>, and surface IgD<sup>-</sup>. We found that up to 3.3% of memory B cells bound to gp120 antigen-specific reagents with the highest frequencies being present in PBMCs, anterior and posterior pelvic LNs, and periaortic LNs (Figure 3, B and C). The lowest frequencies were found in mesenteric LN and terminal ileum samples (range 0.02%–0.23%). Immunizations in this study were administered in the quadriceps, and so it was notable that the frequency of antigen-specific B cells was lower in the putative draining LN site (inguinal) compared with PBMCs, pelvic LNs, and periaortic LNs (Figure 3, B and C).

*Memory B cell repertoire analysis of LN and spleen from RV144 vaccine-immunized RMs.* From sorted memory B cells, we isolated a total of 1,494 mAbs that were screened following transient transfection; 1,242 (83%) of transiently expressed mAbs were reactive with HIV-1 Env (Figure 4A). For RM 22-11, we isolated 76 mAbs from PBMCs only. For the other 2 RMs, we isolated mAbs from PBMCs, spleen, and inguinal, anterior pelvic, posterior pelvic, periaortic and mesenteric LNs and terminal ileum; from terminal ileum we isolated 8 mAbs from RM 46-11 of which 6 were Env reactive, but the single mAb isolated from terminal ileum from RM 60-11 was not Env reactive (Figure 4A). The paucity of Env-reactive B cells in terminal ileum was remarkable given the large number of memory B cells we interrogated from that tissue (Supplemental Table 2). The majority of mAbs were isolated from gp120<sub>AE.A244</sub> Env-sorted cells (Supplemental Table 3), although the recovery of Env-reactive mAbs was similar for gp120<sub>M,Cons</sub> Env-sorted cells; cells sorted using AE.A244 V1V2 tags gave a much lower recovery. We found that Env-reactive antibodies from the RMs had similar isotype (Figure 4B), V<sub>H</sub> gene usage (Figure 4C), and V<sub>L</sub> gene usage (Figure 4, D and E).

**Table 1. Tissue compartment distribution of clonal lineages with 2 or more members**

	Animal ID	
	46-11	60-11
Total Lineages	127	84
PBMC	82 (65%) <sup>^</sup>	22 (26%)
Spleen	52 (65%)	56 (67%)
Inguinal LN	58 (46%)	20 (24%)
Anterior Pelvic LN	32 (25%)	9 (11%)
Posterior Pelvic LN	53 (42%)	19 (23%)
Periaortic LN	2 (2%)	30 (36%)
Mesenteric LN	7 (6%)	17 (20%)
Terminal Ileum	0 (0%)	0 (0%)

<sup>^</sup>Percentages show the fraction of clonal lineages for which members were found in the given tissue. LN, lymph node; PBMC, peripheral blood mononuclear cell.

Isolated Ig genes were analyzed using a Bayesian method (20). The estimated mutation frequency of the heavy chains (HCs) of Env-reactive mAbs was 9.3% (Figure 4F); this mutation frequency was higher than that observed for Env-reactive antibodies isolated from humans immunized 4 times in the GSK PRO HIV-002 trial (3.8%; ref. 21) or in the RV144 trial (2.4%; ref. 17), or for influenza-reactive antibodies recovered from trivalent influenza vaccine recipients (5.8%; ref. 22). To address the possibility that the final immunization induced more somatic hypermutation, we isolated an additional 168 Env-reactive mAbs from PBMCs taken at the week 25 bleed (78 from 22-11, 42 from 46-11, and 48 from 60-11). The mean mutation frequency of this group of mAbs was 5.1% (Supplemental Figure 1A). Comparison of the mutation frequency of mAbs from the 2 time points for each animal was statistically significant (*t* test, *P* < 0.0001 for each animal). This degree of mutation is still higher than that observed in RV144, suggesting that there may be an overestimation of mutation frequency in these RMs, but that the final boost did contribute to additional somatic hypermutation.

Using the same tools, we found that 638 of 1,242 (51%) of Env-reactive antibodies were members of clonal lineages ranging from 2 to 10 members (Figure 5A). For analysis of HC complementarity-determining region 3 (HCDR3) length, we collapsed each clonal lineage so that it would be counted only once; the median HCDR3 length was 16 amino acids for all animals (Figure 5B). This median length was similar to that observed

in the 2 HIV vaccine trials (16.5 amino acids in GSK PRO HIV-002, ref. 21; 15 amino acids in RV144, ref. 17) but shorter than influenza-reactive antibodies (19 amino acids; ref. 22). Longer HCDR3 loops are necessary for some HIV-1 bnAbs to bind to their epitopes (23–27). Interestingly, while no antibodies with HCDR3 loops of 24 amino acids or fewer were found in the 2 human vaccine trials (17, 21), in this study we found that 49 of 1,242 (3.9%) recovered antibodies had HCDR3 loops of that length. Interestingly, the distribution HCDR3 loops of mAbs isolated at week 25 (Supplemental Figure 1B) was not statistically different than the week 55 mAbs (Figure 5B), suggesting that the 6-month rest and fifth immunization did not preferentially expand B cell populations with long HCDR3 loops.

*Tissue distribution of clonal lineages.* From RM 22-11, all 8 clonal lineages were from PBMCs. Five 2-member lineages were directed against the V1V2 loop (Figure 5C), as was one 3-member clonal lineage. One of the 2-member V2-targeted lineages contained a phylogenetically conserved ED motif (12) (lineage DH587), had a 14-amino acid HCDR3, and used V<sub>H</sub> 3~SC11 and V<sub>λ</sub> 3~17 reflective of the putative protective IgG V2 antibodies seen in RV144 (3, 11). Remarkably, one member of this lineage was IgG and the other IgA, suggesting that in RM 22-11 there was the potential for trafficking of both IgA (via polymeric Ig receptor) and IgG (via neonatal Fc receptor) Env-reactive antibodies to mucosal surfaces.

For RM 46-11 and RM 60-11, there were 66 and 50 lineages, respectively, that had exactly 2 members and the majority of these lineages had members that were found in different tissues (50 lineages for RM 46-11, 36 lineages for RM 60-11; Figure 5C). Analysis of the tissue distribution of larger clonal lineages with 3 or more members demonstrated that most lineages shared members across tissue types (Figures 6 and 7). As expected, membership in shared lineages paralleled the recovery of mAbs from tissue sites; the majority of mAbs derived from PBMCs, spleen, and inguinal LNs (Figure 4A), and 88 of 95 (93%) lineages had members from those tissues (Figures 6 and 7). Only 15 of 95 (16%) of lineages shared members with mesenteric LNs and no shared lineage members were isolated from terminal ileum, suggesting that few vaccine-elicited B cells trafficked to those sites.

Interestingly, when we analyzed all clonal lineages with 2 or more members, we found that no single tissue compartment contained members of all clonal lineages (Table 1). Cells from spleen contributed members to approximately two-thirds of lineages and PBMCs contributed to almost half of clonal lineages. These data indicate that studies sampling only peripheral blood may give an incomplete view of clonal lineages elicited by a vaccine in RMs.

*RM mAbs with activities similar to that found in RV144.* Assay of plasma from RV144 participants demonstrated neutralization and ADCC activities (3, 19) and that isolated mAbs recapitulated both activities (17, 19). Of the clonal lineages described above, we selected 4 lineages distributed across multiple tissues that either neutralized HIV-1 or that bound to the surface of HIV-1-infected CD4<sup>+</sup> T cells as required for ADCC, in order to compare these lineages to mAbs isolated from RV144 participants (11, 17, 19) and to determine their detailed binding and/or functional activities.

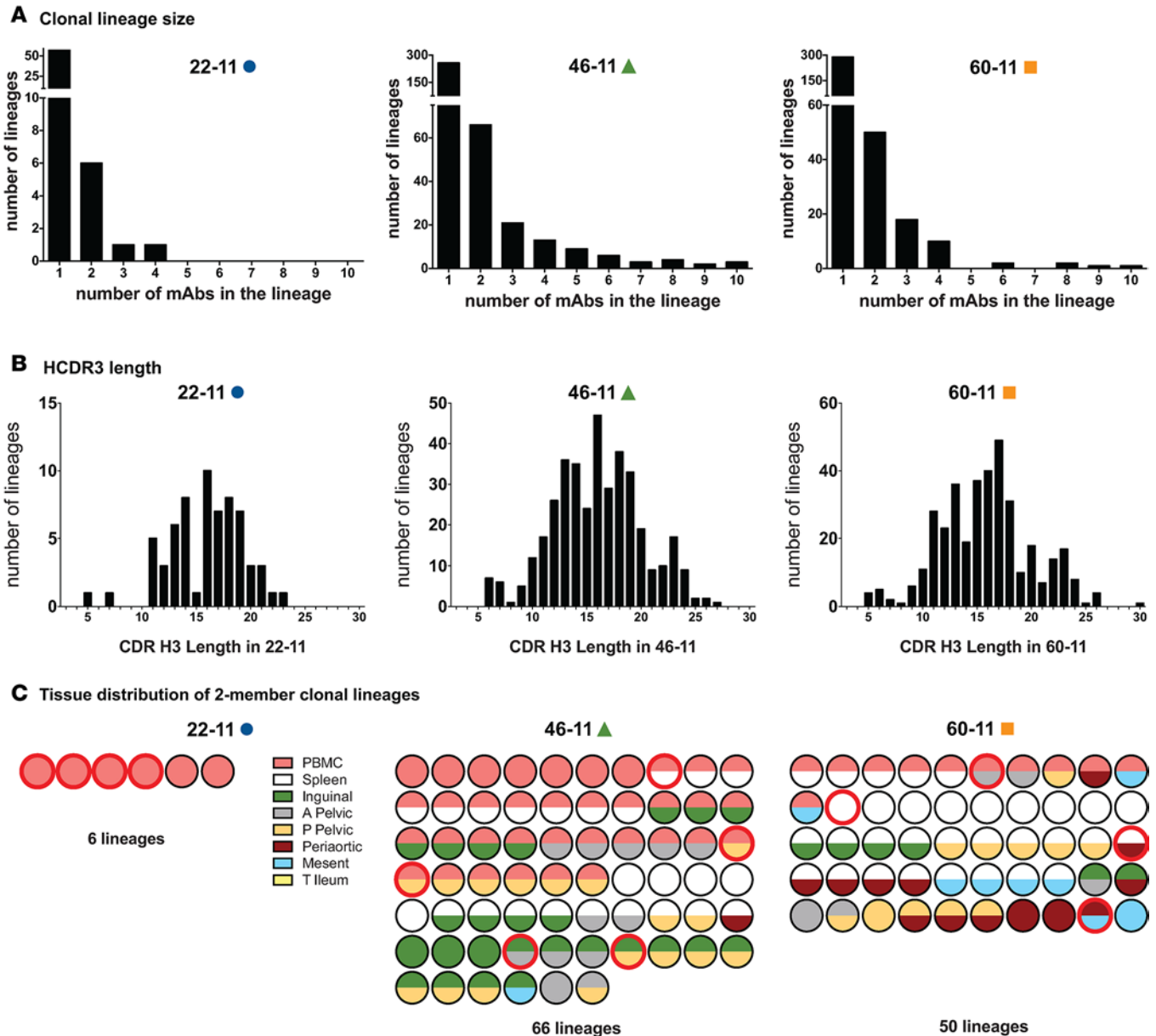


**Figure 5. Clonal lineage characteristics of isolated mAbs.** Analysis of isolated genes demonstrated that many of the mAbs were clonally related. (A) The majority of clonal lineages were comprised of 2 members; larger lineages were detected in each rhesus macaque (RM) up to 4 members for RM 22-11 and up to 10 members for the other 2 animals. (B) For display of heavy chain complementarity-determining region 3 (HCDR3) length, each lineage was collapsed so that it was counted once; for each RM the median HCDR3 length was 16 amino acids. (C) Tissue distribution of 2-member clonal lineages are shown with the site of origin displayed by color. Lineages consisting of antibodies that mapped to the V1V2 loop are identified as red circles. A, anterior; P, posterior; T, terminal; PBMC, peripheral blood mononuclear cell.

The 8-member DH614 lineage was found in 5 different anatomic sites, and this lineage used the same lambda chain gene associated with recognition of K169 (12). The unmutated common ancestor (UCA) of this lineage weakly bound the V1V2 tag AE.A244 protein at high antibody concentrations (data not shown) but did not neutralize (Figure 8A). The mature antibodies of this lineage very potently bound Env proteins and V1V2 tags, but these antibodies did not bind gp120<sub>AE.703357</sub>, an Env protein derived from one of the placebo group infections in the RV144 trial that has a glutamine at position 169 (Q169) (11). All members of this lineage have the glutamic acid/aspartic acid (ED) motif described for other antibodies of this class (12). All mature lineage members potently bound Env proteins and AE.CM235-infected cells; however, neutralization potency varied among the members (Figure 8A).

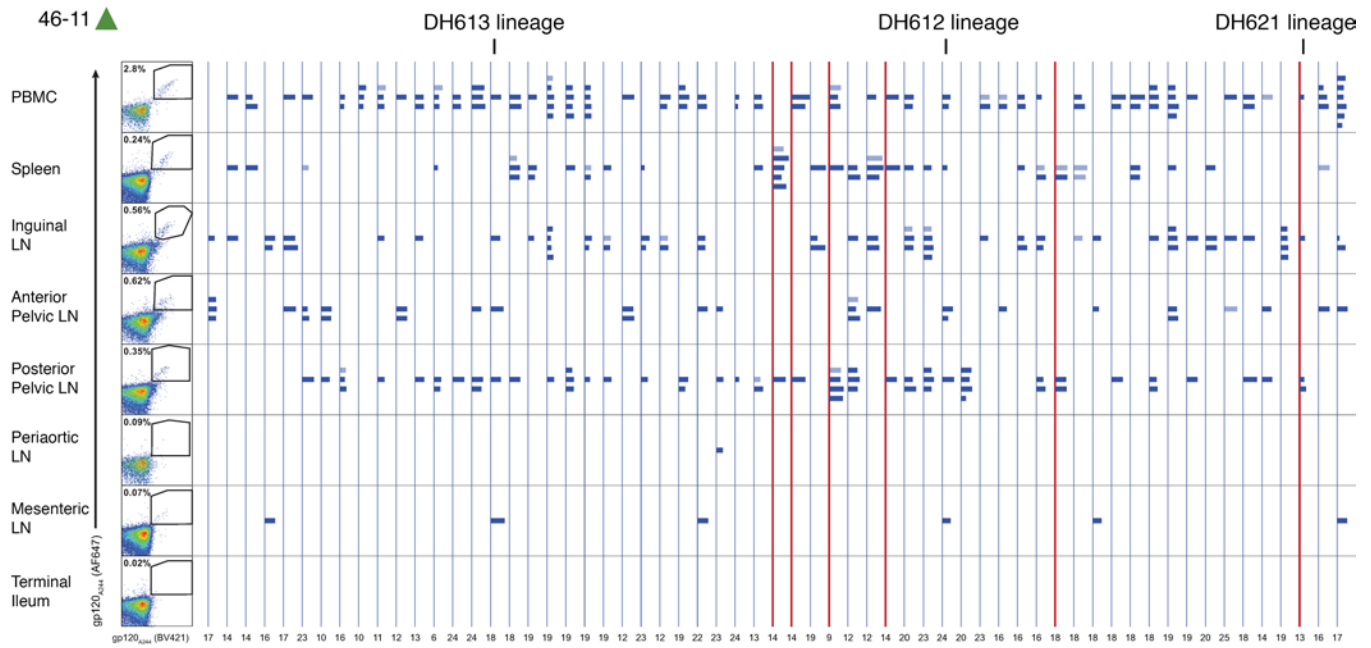


**Figure 6. Tissue distribution of clonal lineages of 3 or more members from rhesus macaque 46-11.** Clonal lineages are displayed in vertical stripes; below the line is shown the heavy chain complementarity-determining region 3 (HCDR3) length as an integer below and the  $V_H$  gene used by the lineage. Lineages that used light chain lambda gene segment  $V_{\lambda}3\sim 17$  are indicated by a dagger ( $\dagger$ ) symbol. Lineages with members that mapped to the V1V2 loop are shown by a red vertical line. Individual mAbs are shown by horizontal tick marks; the length of the tick mark is proportional to heavy chain mutation frequency. Antibodies that were negative for HIV-1 envelope reactivity in screening are shown in light blue. Stripes corresponding to clonal lineages in Figures 8 and 9 are indicated. All clonal lineage mAbs were IgG. No clonal lineages had mAbs isolated from terminal ileum. LN, lymph node; PBMC, peripheral blood mononuclear cell.

In contrast, when tested for neutralization the mature members of the DH612 B cell lineage potentially neutralized the clade B isolate B.MN.3 and more weakly neutralized the clade AE isolate AE.92TH023.6 (Figure 8B); these antibodies were not able to neutralize AE.427299.c12 or AE.CM244.ec1 (data not shown). Antibodies of this lineage bound to AE.CM235-infected target cells (Figure 8B). The 7-member DH612 lineage was distributed across 5 tissues and had a UCA that weakly bound to a V3 tag AE.A244 protein at high antibody concentrations (data not shown). The mature lineage members bound gp120<sub>M,ConS</sub> in ELISA but did not bind a panel of clade AE proteins or V1V2 epitopes in ELISA (Figure 8B), suggesting they recognized a conformational epitope expressed on infected cells.

The 5-member DH613 lineage was found in 5 different anatomic sites, and similar to the DH612 lineage, the DH613 lineage UCA bound to gp120<sub>M,ConS</sub> with an EC50 of 64  $\mu\text{g}/\text{ml}$  but did not neutralize. The mature mAbs of this lineage potentially bound both gp120<sub>M,ConS</sub> and several clade AE gp120 proteins (Figure 8C); however, this lineage bound more weakly to AE.CM235-infected target cells. This lineage potentially neutralized AE.92TH023.6 while still neutralizing B.MN.3, and may be reflective of tier 1 neutralizing antibodies that correlated with decreased infection risk in RV144 (5). The DH612 and DH613 lineages were not directed against the V1V2 loop, and these data combined with the previously reported V1V2-directed mAbs (12) demonstrate that RMs are capable of mounting a multiple-epitope, cross-clade response to the ALVAC/AIDS VAX B/E regimen.

*Epitope mapping of mAbs.* We further analyzed DH614 B cell lineage V2 mAbs on a series of V1V2 peptides that contained amino acid mutations across the 22-amino acid sequence. All mAbs in this lineage were sensitive to mutations at K169 (Figure 9A), consistent with the ED motif described above; these mAbs were sensitive to changes in H173 that was also identified as part of epitope for this class of antibodies (12). CH58 is a human mAb derived from an RV144 trial participant (11) that was sensitive to changes at both K169 and H173, and also to changes at K168, K171, F176, Y177, K178, D180, and P183; the mAbs of the DH614 lineage showed sensitivity to all of these changes except P183, but the degree of sensitivity varied between members of this lineage (Figure 9A), demonstrating ongoing affinity changes. These

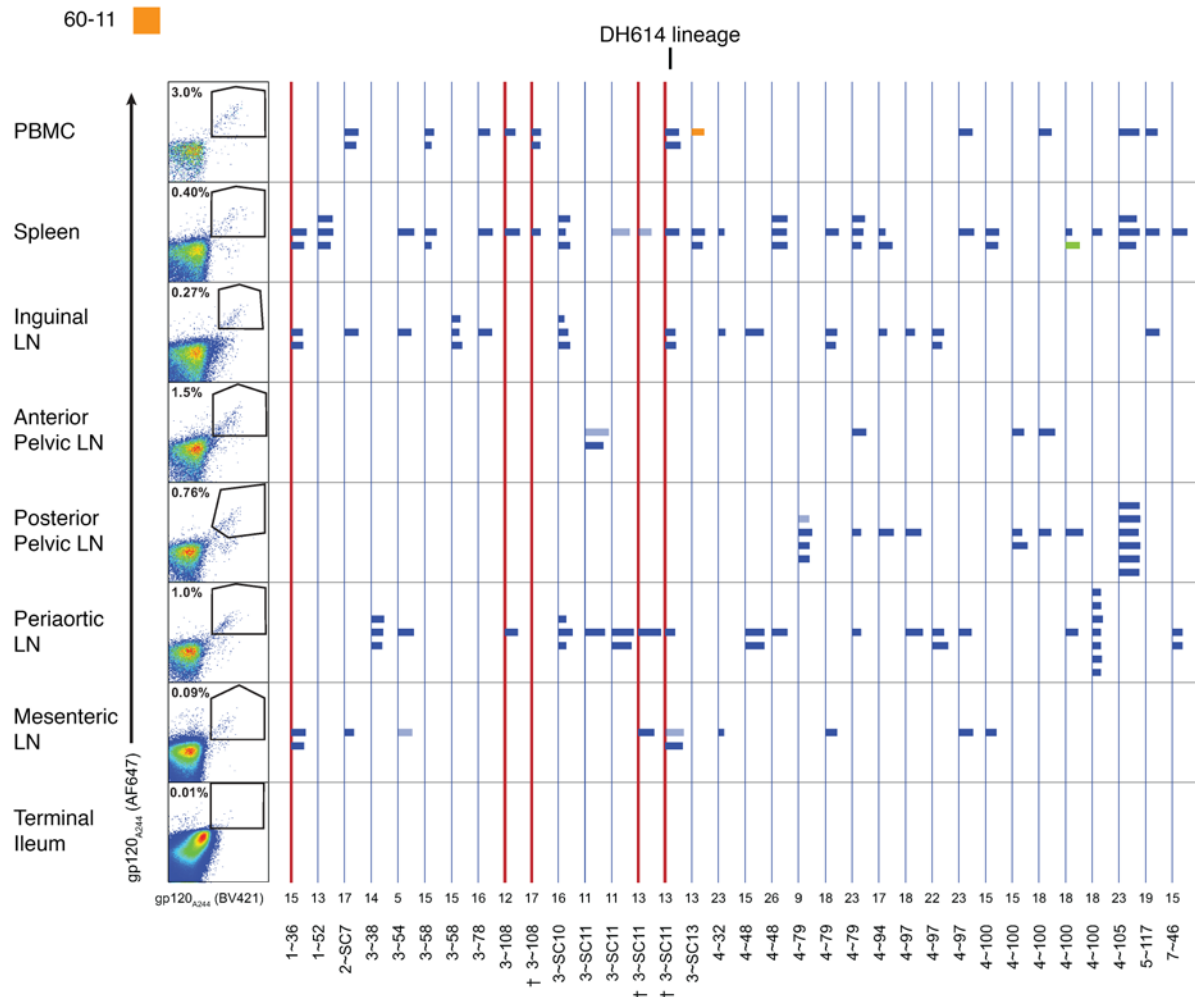


**Figure 7. Tissue distribution of clonal lineages of 3 or more members from rhesus macaque 60-11.** As in Figure 6, clonal lineages are displayed in vertical stripes; below the line is shown the heavy chain complementarity-determining region 3 (HCDR3) length as an integer below and the  $V_H$  gene used by the lineage. Clonal lineage mAbs were IgG except for 1 IgA (orange tick) and 1 IgM (green tick). Lineages that used light chain lambda gene segment  $V_{\lambda}3-17$  are indicated by a dagger ( $\dagger$ ) symbol. Lineages with members that mapped to the V1V2 loop are shown by a red vertical line. Individual mAbs are shown by horizontal tick marks; the length of the tick mark is proportional to heavy chain mutation frequency. Antibodies that were negative for HIV-1 envelope reactivity in screening are shown in light blue. The stripe corresponding to lineage DH614 in Figures 8 and 9 is indicated. No clonal lineages had mAbs isolated from terminal ileum. LN, lymph node; PBMC, peripheral blood mononuclear cell.

mAbs were similar to 2 other  $V_{\lambda}3-17$  antibodies that were not clonally related to each other or to any other mAb isolated (Figure 9D). These mAbs also had the conserved ED motif (12), bound to the surface of AE.CM235-infected cells, and did not bind to the RV144 isolate AE.703357 that did not match the vaccine Env sequence at position 169.

The 4-member DH621 lineage was found in 3 anatomic sites and epitope mapping showed that this lineage was specific for V1V2 and potently bound to AE.CM235-infected cells, but the DH621 lineage had a different pattern of sensitivity to amino acid substitution (Figure 9B) compared with the DH614 lineage (Figure 9A). We also mapped 2 other V1V2 mAbs that were not members of clonal lineages (DH623, DH624) and an additional mAb (DH627) that was clonally related to the previously reported mAb 2554 (12) (Figure 9C); these mAbs also had different V2 reactive patterns compared with other V1V2 mAbs. Notably, DH624 displayed less sensitivity to mutation of H173 (Figure 9C); all of these antibodies bound to AE.CM235-infected cells, suggesting that the diversity of V1V2 responses that we observed might provide overlapping coverage of this variable Env region.

*Antibodies with long HCDR3 loops.* As noted above, we found antibodies with HCDR3 loops longer than those isolated from human HIV-1 vaccine trials. Since a number of HIV-1 bnAbs have long HCDR3 loops, we sought to determine if these antibodies from RMs had characteristics suggestive that they might be

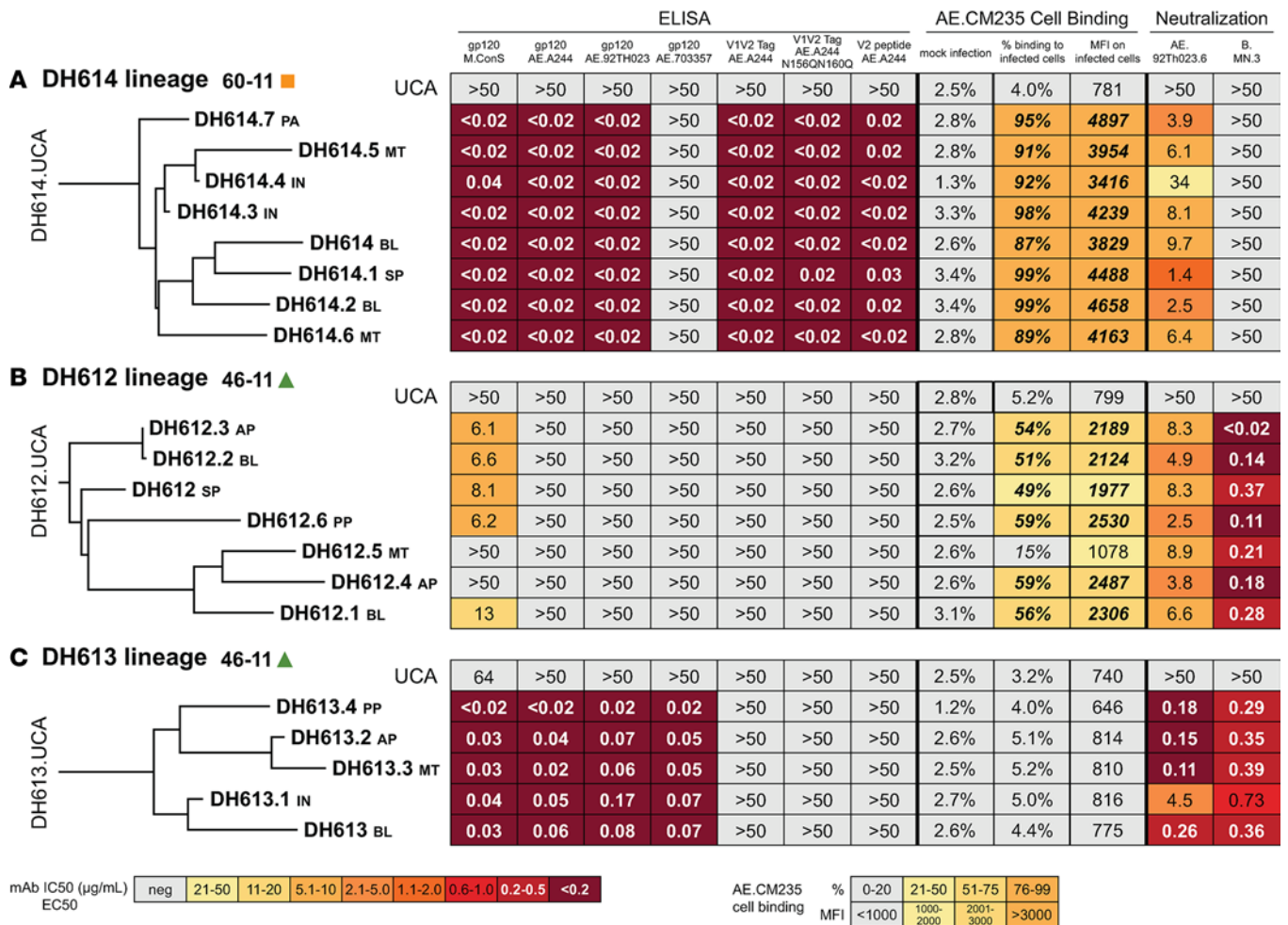


**Figure 8. Clonal lineages of isolated mAbs.** Phylograms of clonal lineages isolated from rhesus macaques (RMs) are shown with antibody data on each line to the right of the mAb name. **(A)** Mature lineage DH614 potently bound to gp120 proteins and V1V2 targets with the exception of RV144 breakthrough strain gp120<sub>AE.703357</sub>; the lineage members also neutralized AE.92TH023.6 and the mature antibodies bound to the surface of AE.CM235-infected target cells. Lineage characteristics: V<sub>H</sub>3~5C11/J<sub>H</sub>4, heavy chain (HC) complementarity-determining region 3 (HCDR3) length 13, mean HC mutation frequency 10.4%; V<sub>L</sub>3~17/V<sub>L</sub>2 CDR3 length 10, mean light chain (LC) mutation frequency 5.9%. **(B)** Mature lineage DH612 mAbs bound to gp120<sub>M.Cons</sub> and neutralized B.MN.3 but did not bind or neutralize clade AE targets. The mature mAbs bound to the surface of AE.CM235-infected target cells. Lineage characteristics: V<sub>H</sub>4~82/J<sub>H</sub>6, HCDR3 length 24, mean HC mutation frequency 8.4%; V<sub>K</sub>1-LC1c/J<sub>K</sub>2, CDR3 length 9, mean LC mutation frequency 9.2%. **(C)** Mature lineage DH613 mAbs potently bound gp120 proteins from clade AE and group M consensus but did not bind V1V2-specific targets. The mature antibodies potently neutralized both AE.92TH023.6 and B.MN.3; the mature antibodies weakly bound to AE.CM235-infected target cells. Lineage characteristics: V<sub>H</sub>3~5C11/J<sub>H</sub>4, HCDR3 length 18, mean HC mutation frequency 11.1%; V<sub>K</sub>1~23/J<sub>K</sub>1, CDR3 length 9, mean LC mutation frequency 4.4%. The anatomic site of origin appears after the mAb name: BL, peripheral blood; SP, spleen; IN, inguinal lymph node (LN); AP, anterior pelvic LN; PP, posterior pelvic LN; PA, periaortic LN; MT, mesenteric LN. Data are in µg/ml, color coded as shown in the legend for ELISA half maximal effective concentration (EC50) and neutralization inhibitory dilution 50% (ID50), or as % cell binding. MFI, mean fluorescence intensity; UCA, unmutated common ancestor.

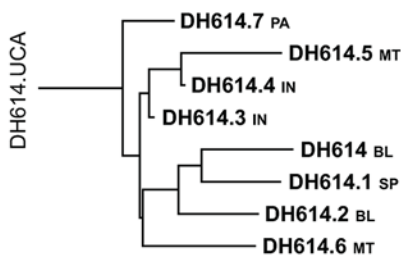
precursors of bnAbs; we examined 8 of the 49 Env-reactive mAbs with HCDR3 loops of 24 or more amino acids (Figure 9E). These mAbs were isolated from multiple anatomic sites and displayed an array of binding patterns. While some of the antibodies were sensitive to the loss of the N332 glycosylation site, none of the mAbs displayed potent neutralization (data not shown); mAb DH606 neutralized AE.92TH023.6 with an EC50 of 3.9 µg/ml and B.MN.3 at 0.48 µg/ml. DH606 and 3 other mAbs bound to AE.CM235-infected cells, suggesting that some of these long HCDR3 mAbs may have been developing the ability to mediate anti-HIV-1 functions after the fifth boost.

## Discussion

In this study we have probed the RM plasma response to the ALVAC/AIDSVAX B/E gp120 vaccine and the memory B cell repertoire found in circulation and in lymphoid and mucosal tissues. The RMs in this study all developed robust plasma responses following vaccination that were sustained during

**A DH614 lineage**

60-11 ■



WT	L	R	D	K	K	Q	K	V	H	A	L	F	Y	K	L	D	I	V	P	I	E	D
>50	>50	>50	>50	>50	>50	>50	>50	>50	>50	>50	>50	>50	>50	>50	>50	>50	>50	>50	>50	>50	>50	>50
0.02	0.90	0.75	0.58	1.5	47	0.88	1.2	0.05	>50	0.61	0.45	38	12	1.2	0.53	1.7	0.68	0.80	0.77	0.79	0.60	0.71
0.59	0.37	0.68	0.64	1.2	20	0.78	0.86	0.60	3.7	0.71	0.43	0.65	4.0	1.1	0.54	1.3	0.60	0.70	0.72	0.81	0.53	0.66
2.5	1.7	3.3	3.1	6.1	>50	3.6	4.8	4.2	>50	3.1	2.3	>50	>50	4.5	2.5	7.1	3.3	3.5	4.2	3.9	3.1	2.9
0.20	0.13	0.25	0.22	0.42	>50	0.29	0.32	0.21	>50	0.42	0.15	>50	2.1	0.36	0.20	0.55	0.25	0.31	0.25	0.37	0.25	0.23
0.33	0.35	0.38	0.34	0.53	14	0.39	0.51	0.29	9.5	0.41	0.35	1.7	0.85	0.52	0.35	0.67	0.47	0.48	0.46	0.52	0.40	0.43
0.39	0.33	0.43	0.37	0.68	12	0.43	0.55	0.35	>50	0.42	0.31	>50	2.7	0.63	0.31	0.80	0.42	0.46	0.43	0.62	0.35	0.41
0.35	0.28	0.39	0.30	0.35	13	0.42	0.37	0.29	>50	0.37	0.27	>50	0.52	0.60	0.31	0.73	0.42	0.49	0.42	0.53	0.32	0.34
0.34	0.32	0.50	0.40	0.34	5.5	0.48	0.51	0.37	16	0.44	0.33	0.81	1.1	0.65	0.35	0.85	0.53	0.48	0.46	0.61	>50	0.42

**B DH621 lineage**

46-11 ▲



WT	L	R	D	K	K	Q	K	V	H	A	L	F	Y	K	L	D	I	V	P	I	E	D
27	21	32	17	>50	44	>50	>50	20	>50	8.2	>50	>50	18	>50	21	>50	24	29	24	17	23	19
14	16	16	13	29	20	17	22	15	>50	9.8	11	6.8	13	>50	16	36	18	17	16	12	16	15
23	21	29	18	>50	44	>50	>50	>50	>50	31	5.3	3.4	>50	>50	23	>50	34	29	27	21	33	28
ND	ND	ND	ND	ND	ND	ND	ND	ND	ND	ND	ND	ND	ND	ND	ND	ND	ND	ND	ND	ND	ND	ND

AE.CM235 Cell Binding		
mock infection	% binding to infected cells	MFI on infected cells
4.7%	71%	2584
4.7%	94%	3902
3.5%	98%	4846
2.2%	90%	3632

**C Non-V<sub>3</sub>~17 V1V2 mAbs**

- DH623 AP ▲ V<sub>H</sub>4~100 / J<sub>H</sub>6, 16 aa, 11.9% // V<sub>K</sub>2~118
- DH624 AP ▲ V<sub>H</sub>2~33 / J<sub>H</sub>4, 10 aa, 7.7% // V<sub>K</sub>1~48
- DH627 PP ▲ V<sub>H</sub>3~SC11 / J<sub>H</sub>4, 11 aa, 10.3% // V<sub>K</sub>2~73

WT	L	R	D	K	K	Q	K	V	H	A	L	F	Y	K	L	D	I	V	P	I	E	D
1.6	1.3	2.2	1.3	3.9	2.7	2.5	2.9	1.8	29	1.2	0.15	0.57	1.2	3.4	0.21	1.2	1.9	1.7	1.8	1.5	1.7	1.5
5.7	4.5	7.3	3.8	18	11	8.5	10	5.5	10	4.4	1.1	0.37	4.7	>50	>50	>50	4.6	3.3	4.9	6.2	5.5	4.3
8.2	6.8	10	4.7	23	14	11	18	6.7	>50	9.6	>50	16	7.3	>50	41	19	7.9	7.3	8.5	6.6	9.4	6.1

AE.CM235 Cell Binding		
mock infection	% binding to infected cells	MFI on infected cells
4.7%	94%	3950
3.9%	62%	2202
3.7%	28%	1504

**D V<sub>3</sub>~17 V1V2 mAbs**

- DH596 IN ▲ V<sub>H</sub>4~96 / J<sub>H</sub>5, 14 aa, 13.4% // V<sub>K</sub>3~17
- DH597 BL ▲ V<sub>H</sub>4~SC6 / J<sub>H</sub>5, 14 aa, 11.8% // V<sub>K</sub>3~17

gp120 M.ConS	gp120 AE.A244	gp120 AE.92TH023	gp120 AE.703357	V1V2 Tag AE.A244	V1V2 Tag AE.A244 N156QN160Q	V2 peptide AE.A244
0.06	<0.02	<0.02	>50	<0.02	<0.02	0.03
4.0	0.02	0.02	15	0.02	0.03	0.03

AE.CM235 Cell Binding		
mock infection	% binding to infected cells	MFI on infected cells
15%	94%	4821
14%	90%	4318

**E Long HCDR3 mAbs**

- DH605 IN ▲ V<sub>H</sub>4~32 / J<sub>H</sub>5, 24 aa, 12.9% // V<sub>K</sub>1~116
- DH606 BL ▲ V<sub>H</sub>4~100 / J<sub>H</sub>5, 25 aa, 13.1% // V<sub>K</sub>1~107
- DH607 SP ▲ V<sub>H</sub>3~SC11 / J<sub>H</sub>5, 27 aa, 7.8% // V<sub>K</sub>1~LC1
- DH608 SP ▲ V<sub>H</sub>4~32 / J<sub>H</sub>6, 26 aa, 10.6% // V<sub>K</sub>2~73
- DH609 SP ▲ V<sub>H</sub>4~48 / J<sub>H</sub>6, 26 aa, 11.2% // V<sub>K</sub>2~73
- DH610 SP ▲ V<sub>H</sub>3~108 / J<sub>H</sub>6, 26 aa, 7.0% // V<sub>K</sub>1~23
- DH611 SP ▲ V<sub>H</sub>4~48 / J<sub>H</sub>6, 26 aa, 11.6% // V<sub>K</sub>2~73
- DH622 MT ▲ V<sub>H</sub>1~90 / J<sub>H</sub>5, 30 aa, 3.7% // V<sub>K</sub>2D~105

AE.A244 gp120							C.YU2 gp120			AE.CM235 Cell Binding		
WT	N156K N160K	N259A N301A N332A	N276A	N278A	Δ371I P363N	D368R	WT	Core	D368R	mock infection	% binding to infected cells	MFI on infected cells
0.50	0.71	2.2	0.72	0.34	0.18	0.41	0.71	>50	9.0	2.5%	4.0%	756
0.04	0.06	0.13	0.05	0.03	0.17	<0.02	0.03	16	0.12	2.5%	74%	3135
>50	>50	>50	>50	>50	>50	>50	0.36	0.19	>50	3.6%	7.8%	840
0.11	0.10	0.14	0.13	0.16	0.16	0.12	1.1	0.22	10	2.6%	3.2%	730
0.18	0.49	0.65	0.36	0.13	2.6	0.04	0.23	0.04	5.9	3.3%	81%	2802
0.04	0.06	0.10	0.07	0.04	0.02	0.05	0.03	0.56	0.26	3.4%	7.6%	734
0.18	0.43	0.84	0.35	0.14	1.7	0.10	0.20	0.51	4.7	3.3%	84%	3076
2.5	1.9	>50	6.2	2.1	>50	0.14	0.14	>50	0.95	3.3%	76%	2142

mAb IC50 (μg/mL)	EC50
neg	21-50
11-20	5.1-10
2.1-5.0	1.1-2.0
0.6-1.0	0.2-0.5
<0.2	

AE.CM235 cell binding	% MFI
0-20	1000-2000
21-50	2001-3000
51-75	>3000
76-99	

**Figure 9. Epitope mapping of mAbs and characterization of mAbs with long HCDR3 loops.** Phylograms for clonal lineages DH614 and DH621 shown with anatomic site of origin. Epitope mapping ELISA data shown as half maximal effective concentration (EC50) and color coded as in the legend. The sequence of the 22-amino acid V2 peptide is shown across the top of the grids (A–C) and data below each amino acid are the observed EC50 for variant peptide constructs with substitutions at that position. (A) Mature lineage DH614 mAbs were most sensitive to changes at K169, H173, F176, and Y177. For this lineage, data for binding to infected cells are shown in Figure 8. (B) Mature lineage DH621 mAbs were most sensitive to changes at K168, Q170, K171, H173, K178, and D180. Lineage members bound the surface of AE.CM235-infected target cells. Lineage characteristics: V<sub>H</sub>5~117/J<sub>H</sub>4, heavy chain (HC) complementarity-determining region 3 (HCDR3) length 13, mean HC mutation frequency 5.2%; V<sub>K</sub>2~73/J<sub>K</sub>4, CDR3 length 9, mean light chain (LC) mutation frequency 4.7%. (C) V1V2-specific mAbs that did not use V<sub>3</sub>~17 showed different patterns of sensitivity to amino acid substitutions. DH623 showed significantly reduced binding only for changes at H173. DH624 was not sensitive to H173 changes but was sensitive to changes at K178, L179, and D180. DH627 was sensitive to changes at H173, L175, and K178. All 3 mAbs bound the surface of AE.CM235-infected target cells. (D) Two mAbs that did use V<sub>3</sub>~17 did not bind to gp120 from RV144 breakthrough strain AE.703357, but did bind to proteins and V1V2 proteins reflective of the vaccine, and also bound to AE.CM235-infected target cells. (E) Tested long HCDR3 mAbs showed 3 patterns of binding to gp120 constructs. DH605 and DH622 showed reduced binding to gp120<sub>AE.A244</sub>, N259A/N301A/N332A. DH609 and DH611 were clonally related and showed reduced binding to gp120<sub>AE.A244</sub>, Δ371I/P363N and gp120<sub>C.YU2</sub> D368R; DH607 did not bind clade AE proteins but was sensitive to gp120<sub>C.YU2</sub> D368R. DH606, DH608, and DH610 potentially bound all tested variants of gp120<sub>AE.A244</sub> but differentially bound gp120<sub>C.YU2</sub> variants. The anatomic site of origin appears after the mAb name: BL, peripheral blood; SP, spleen; IN, inguinal lymph node (LN); AP, anterior pelvic LN; PP, posterior pelvic LN; PA, periaortic LN; MT, mesenteric LN; ND, not done; MFI, mean fluorescence intensity; UCA, unmutated common ancestor.

the 30-week rest (Figure 1, G–L), but interestingly the plasma blocking activity and neutralization waned more than overall binding activity, although both activities rose after the final boost to levels comparable to those observed after the first 4 immunizations (Figure 1, B–F, and Figure 2, A–E). While this waning could be partially explained by differences in assay sensitivity and detection limits, the observed differences in functional assays is also consistent with different kinetics for the components of this polyclonal vaccine response, as might be expected if they arise from different pools of B cells. As with the human RV144 trial (19), neutralization breadth elicited by ALVAC/AIDSVAX immunization in RMs was modest, with titers similar between the fourth and fifth immunization time points (Figure 2, A–E); all animals also developed plasma antibodies that mediated ADCC after the fourth immunization (Figure 2, F–N). We found evidence of systemic V1V2 antibodies (Figure 1, J and K) of the type that correlated with decreased risk in the RV144 vaccine trial (3, 6). All of these data suggest that the regimen in RMs elicited antibody levels and functions that were similar to those observed in the human trial.

We selected a subset of animals for a more detailed anatomic analysis, and found that antigen-specific B cells could be detected in all sampled tissues (Figure 3). Specifically, we isolated B cells expressing V2 K169 antibodies that mediated tier 1 neutralization and bound infected cells, along with V3 and CD4 binding site-directed antibodies with specificities similar to those of antibodies isolated from RV144 participants (11, 17, 19). Importantly, these antibodies circulated in inguinal and pelvic LNs and spleen but were not found in terminal ileum. However, IgG Env antibodies were found in rectal wash fluids, indicating that the antibodies likely were derived from plasma/tissue fluid antibodies that crossed the mucosal barrier rather than being produced locally by intestinal mucosal B cells. Prior work on intestinal biopsies from early HIV-1 infection patients found that gp120-reactive B cells were not present, but gp41-reactive B cells could be found that cross-react with intestinal microbiota-derived antigens (28). The AIDS VAX B/E vaccine did not contain gp41 and the ALVAC component contained only the transmembrane anchoring portion of gp41, and so the lack of gp120-reactive B cells found in terminal ileum in the present study may be because the vaccine-elicited B cells could not home to those mucosa-associated lymphoid tissues or because cells that did home to those sites were short-lived. We did not directly sample either vagina or rectum; thus, we do not know if antibody-secreting cells were present at those sites, but the rectal antibody data (Figure 1, M–R) do not suggest that long-lived plasma cells were present and secreting Env-specific antibodies prior to the final boost. These RMs were immunized in the quadriceps and so it was interesting that the likely draining LN site (inguinal LN) did not have the highest frequency of antigen-specific B cells. Both anterior and posterior pelvic LNs had frequencies of antigen-specific B cells similar to that of PBMCs (Figure 3, B and C), and it is possible that B cells in these LNs could be rapidly recruited to sites of sexual transmission of HIV-1 (vagina and rectum) at the time of exposure, but whether this would have an impact on infection risk is not known.

We were able to detect rectal fluid antibodies in all animals after the fourth immunization time point (week 26), but in most RMs these antibodies waned to below the limit of detection during the 30-week rest (Figure 1, M–R). Immediately prior to necropsy after the final immunization, we did not detect rectal antibody in 2 of the 5 animals, despite those animals having detectable antibodies at earlier time points. The heterogeneity of rectal antibody responses and the profound waning observed may provide an insight into the modest protective efficacy observed in the RV144 trial.

In addition, data from this anatomic study suggest that examination of peripheral blood may give only a partial view of the richness of B cell responses to a vaccine. We observed that clonal lineages were shared among many tissues (Figures 5C, 6, and 7) but only ~45% of these lineages had members found in peripheral blood (Table 1). Given recent work aimed at stimulating germline precursors of broadly neutralizing antibodies and quantifying those responses (29–31), data from the present study suggest that sampling of blood alone may not be able to detect all vaccine-elicited responses.

In summary, these results show that the RV144 regimen in RMs elicited a response similar to that observed in humans, and that this response was epitopically diverse and anatomically distributed. Mucosal antibodies were present but waned over the 30-week rest, consistent with the decreasing protection observed in the human trial. Our results suggest that the RV144 regimen in humans likely did not induce antigen-specific B cell trafficking to intestinal mucosae.

## Methods

**Immunization of RM subjects.** The vaccine regimen for this study is shown in Figure 1A. In short, ALVAC vCP1521 ( $5 \times 10^7$  PFU per dose) was administered in the quadriceps at weeks 0 and 4. Boosting immunizations of  $5 \times 10^7$  PFU per dose ALVAC vCP1521 plus 600  $\mu\text{g}$  per dose of AIDS VAX B/E gp120 were given at weeks 12, 23, and 53. Peripheral blood was obtained at each immunization and 2 weeks after each immunization. Rectal antibodies were sampled by a surgical sponge placed in the rectum at weeks 25, 29, 53, and 55. Two weeks after the week 53 boost, the animals were euthanized and peripheral blood, spleen, inguinal LN, anterior pelvic LN, posterior pelvic LN, periaortic LN, mesenteric LN, and terminal ileum were collected. Peripheral blood was processed for serum (coagulated blood) or plasma and PBMCs (anticoagulated blood); all samples were aliquoted and maintained at  $-80^\circ\text{C}$  (serum/plasma) or in liquid nitrogen vapor phase (cells) for further analysis.

**Single-cell flow cytometry sorting.** Isolated cells were stained with a panel of fluorochrome-antibody conjugates and reagents to identify antigen-specific memory B cells. The panel consisted of Aqua Vital dye (Life Technologies); CD3 (peridinin chlorophyll protein-cyanine dye 5.5 [PerCP-Cy5.5], clone SP34-2), CD16 (phycoerythrin [PE]-Cy7, clone 3G8), CD20 (FITC, clone L27) (all BD Biosciences); CD14 (Brilliant Violet [BV] 570, clone M5E2), CD27 (allophycocyanin [APC]-Cy7, clone O323) (both Biolegend); and IgD (PE, catalog 2030-09) (Southern Biotech). Preformed conjugates for antigen-specific B cell sorting were made as described (21) using streptavidin conjugated to AlexaFluor 647 (Life Technologies) or BV421 (Biolegend). Antigen-specific probes were made using gp120<sub>AE.A244</sub>, gp120<sub>M.ConS</sub>, and AE.A244 V1V2 tags (11). Memory B cells were defined as CD3<sup>+</sup>/14<sup>+</sup>/16<sup>-</sup>, CD20<sup>+</sup>, and surface IgD<sup>-</sup>; antigen-specific memory B cells positive for probes in both colors were sorted as single cells into 96-well plates containing 20  $\mu\text{l}$ /well reverse transcriptase (RT) buffer (Invitrogen) as described (32). Sorted plates were frozen immediately and maintained at  $-80^\circ\text{C}$  before RT/PCR.

**PCR amplification of immunoglobulin  $V_H$  and  $V_L$  genes.** The  $V_H$  and  $V_L$  genes of sorted single memory B cells were amplified as described (12, 32). A  $65^\circ\text{C}$ , 5-minute pre-RT incubation was performed by adding 0.1  $\mu\text{M}$  of a mixture of Ig constant region primers (including IgA, IgM, IgD, IgG, and IgE) to each well. Samples were chilled on ice and RT buffer was added following a  $50^\circ\text{C}/45$ -minute,  $55^\circ\text{C}/15$ -minute RT/PCR reaction. First round PCR (PCRa) of heavy, kappa, and lambda chains was then performed using the cDNA product of RT/PCR. Each 50- $\mu\text{l}$  reaction contained 5  $\mu\text{l}$  cDNA, 0.6  $\mu\text{l}$  HotStar Taq (Qiagen), 5  $\mu\text{l}$  PCR Buffer (Qiagen), 10  $\mu\text{l}$  Q Buffer (Qiagen), 0.4  $\mu\text{l}$  25 mM dNTPs (Qiagen), 25 mM  $\text{MgCl}_2$  (1  $\mu\text{l}$  for IgH, 2  $\mu\text{l}$  for Ig $\kappa$  and 3  $\mu\text{l}$  for Ig $\lambda$ ), and 0.125  $\mu\text{M}$  IgH, Ig $\kappa$ , or Ig $\lambda$  variable region primer mixtures. PCRa reaction conditions were as follows:  $95^\circ\text{C}/5$  minutes, ( $94^\circ\text{C}/30$  seconds,  $62^\circ\text{C}$  [for IgH] or  $64^\circ\text{C}$  [for Ig $\kappa/\lambda$ ]/45 seconds,  $72^\circ\text{C}/90$  seconds) for 35 cycles,  $72^\circ\text{C}/7$  minutes, then hold at  $10^\circ\text{C}$ .

PCRa products were used as templates for nested PCR (PCRb). Each 50- $\mu\text{l}$  reaction contained 3  $\mu\text{l}$  PCRa product, 0.6  $\mu\text{l}$  HotStar Taq (Qiagen), 5  $\mu\text{l}$  PCR Buffer, 10  $\mu\text{l}$  Q Buffer, 0.4  $\mu\text{l}$  25 mM dNTPs, 25 mM  $\text{MgCl}_2$  (3  $\mu\text{l}$  for IgH, 2  $\mu\text{l}$  for Ig $\kappa/\lambda$ ) and 0.125  $\mu\text{M}$  IgH, Ig $\kappa$ , or Ig $\lambda$  internal primers. PCRb reaction conditions were the same as for PCRa above. PCRb products were then analyzed by 1.2% SYBER Safe E-Gels (Invitrogen). Wells with bands indicating a PCR product were purified and sequenced. Sequencing results were analyzed by SoDA (33) and ARPP (20) software to infer VDJ arrangements.

Analysis of RM genes and clonal lineages was performed as described (12, 20, 34). Clonal lineage membership was determined using Cloanalyst (20, 34, 35).

**Recombinant mAb expression.** For high-throughput characterization of isolated mAbs, transient transfection was performed as previously described (12, 32). To produce the transfection construct, 2  $\mu\text{l}$   $V_H/V_L$  PCRb product, 1  $\mu\text{l}$  KOD polymerase (Novagen), 5  $\mu\text{l}$  KOD buffer, 5  $\mu\text{l}$  dNTPs, 3  $\mu\text{l}$  25 mM  $\text{MgSO}_4$ , 1  $\mu\text{l}$  CMV-262, 1  $\mu\text{l}$  1822BGH (IgH) or BGH-1235 (Ig $\kappa/\lambda$ ), 2  $\mu\text{l}$  rhesus CMV\_P DNA fragments, 2  $\mu\text{l}$  reversed DNA primers for either IgH or Ig $\kappa/\lambda$  were brought to 50  $\mu\text{l}$  with  $\text{H}_2\text{O}$ . PCR conditions were as follows:  $95^\circ\text{C}/2$  minutes, ( $95^\circ\text{C}/20$  seconds,  $62^\circ\text{C}/12$  seconds,  $70^\circ\text{C}/60$  seconds) for 30 cycles, then hold at  $4^\circ\text{C}$ . PCR products were purified by MinElute 96UF plates and analyzed by QIAxcel (Qiagen) before transient transfection.

Transient transfection was performed using 293T cells cultured in 6-well plates. Approximately 1  $\mu\text{g}$  of heavy and light chain recombinant linear fragments was cotransfected by Effectene (Qiagen) when cells cultured in 10% FBS supplemented DMEM were 80%–90% confluent. Cell medium was changed to 2% FBS/DMEM before adding the transfection mixture. After 3 days of incubation at  $37^\circ\text{C}/5\%$   $\text{CO}_2$ , supernatants were harvested for analysis.

For large-scale production of mAbs, isolated  $V_H$  and  $V_L$  genes were cloned into pcDNA3.1(+) plasmid containing the CMV promoter and IgG constant regions (GenScript). Plasmids were amplified by Plasmid Plus Mega kit (Qiagen) and concentrated.  $V_H$  and  $V_L$  plasmids were cotransfected into 293i cells by PEI transfection reagent (EMD Millipore). Medium was changed to FreeStyle 293 Expression Medium (ThermoFisher) 6 hours after transfection. Cells were cultured on a shaker at 120 rpm, 37°C, and 8%  $CO_2$ . After 5 days of incubation, supernatants were harvested and mAbs purified by Protein A agarose beads (ThermoFisher). SDS-PAGE and Western blots under reducing and nonreducing conditions were used to analyze antibody quality (32).

*ELISA assays of RM plasma and antibodies.* Plasma from each RM at week 0, 4, 6, 14, 25, 53, and 55 were heat inactivated at 56°C for 5 minutes before assay by ELISA. HIV-1 antigens included the panel previously described (11): gp120<sub>AE.A244</sub> (including the WT strain and the mutants K169V and K169V/V172E/H173Y); gp120<sub>AE.703357</sub> (WT, Q169K, mut3); gp120<sub>AE.427299</sub> (WT, Q169K, mut4); gp120<sub>92Th023</sub> (WT, N160K); gp120<sub>B,MN</sub>; AE.A244 V1V2 tags (WT, N156Q/N160Q); gp70 Case A V1V2 (WT, 169K, mut3); and MuLV gp70 as a negative control. Antigens were coated at 4°C on 384-well Costar high-binding ELISA plates at 30 ng per well. After overnight incubation, ELISA plates were blocked by Superblock (40 g whey protein, 150 ml goat serum, 5.0 ml Tween-20, 0.5 g  $NaN_3$ , and 40 ml 25× PBS brought to 1 liter with deionized water) for 1 hour at room temperature. Plasma was diluted 3-fold for 12 dilutions in Superblock buffer and added at 10  $\mu$ l per well. After the 1-hour room temperature incubation, plates were washed twice with PBS containing 0.1% Tween-20. Horseradish peroxidase-conjugated goat anti-monkey secondary antibodies (Rockland, catalog 617-103-012) were diluted 1:10,000 in Superblock and added at 10  $\mu$ l per well for a 1-hour incubation. Plates were washed 4 times before 20  $\mu$ l of SureBlue Reserve TMB-1 Solution (KPL) was added. After a 15-minute incubation, the reaction was stopped with 20  $\mu$ l 1% HCl. Plates were read by a SpectraMax Plus 384 plate reader (Molecular Devices) at 450 nm. Area under the curve was calculated using the trapezoidal method.

Competitive inhibition ELISAs were performed as previously described (36) using the same plasma samples at 1:50 dilution and using gp120<sub>AE.A244</sub> as the target antigen. HIV-1 mAbs A32 (37), CH01 (18), CH58 and CH59 (11), as well as sCD4, were tested.

For  $V_H$  and  $V_L$  transient transfection supernatants, screening was performed as described (11, 32) using the following HIV-1 antigens: gp120<sub>AE.A244</sub> (WT, N160K); gp120<sub>M,ConS</sub>; gp120<sub>AE.703357</sub> (WT); gp120<sub>AE.427299</sub> (WT); gp120<sub>B.9021</sub>; gp120<sub>B,MN</sub>; gp120<sub>C.1086</sub>; AE.A244 V1V2 tags (WT, N156Q/N160Q); gp70 Case A V1V2 (WT, 169K); gp70 AE.A277\_92TH23 V3; gp70 B.MN V3; and biotinylated clade AE Env constant region 1 (C1) peptide. The mAb concentration in each supernatant was quantified using a capture ELISA method as previously described (38); known concentrations of mAb 2F5 were used to generate the standard curve. Supernatants were undiluted for ELISA binding screening. For mAbs produced at larger scale and purified, the same antigens were tested. For V2 mAb epitope mapping, a panel of alanine-scanning peptides based on the AE.A244 V2 sequence spanning from L165 to D186 (LRDKKQKVHALFYKLDIVPIED) was used (11). Concentrations of mAbs were determined by Nanodrop and tested using 3-fold dilutions 12 times starting at 100  $\mu$ g/ml; ELISA was performed as described above.

*Rectal HIV-1-specific antibody assay.* HIV-1-specific antibodies were measured by RM BAMA for total and Env-specific IgG antibodies in rectal Weck-Cel sponges. Specific activity was calculated by dividing the antibody binding units by the total IgG concentration as previously described (39).

*Neutralization assay of sera and antibodies.* Serum samples from weeks 0, 14, 25, 53, and 55 were tested for neutralization activity, as were purified mAbs produced as described above. Pseudotyped virus strains including B.MN.3, C.MW965.26, B.SF162.LS, B.BaL.26, and AE.92Th023.6, as well as simian virus amphotropic murine leukemia virus (SVA-MVA) as a control, were tested using TZM-bl cells (40). Serum samples were heat inactivated at 56°C for 5 minutes before testing; testing was done on samples diluted 3-fold (8 dilutions) starting at a 1:20 dilution for sera or 50  $\mu$ g/ml for mAbs. Inhibitory dilution 50% (ID50) as reciprocal dilution for serum neutralization activity and  $IC_{50}$  as  $\mu$ g/ml for mAb neutralization activity were calculated using logistic regression.

*Surface plasmon resonance analysis of antibody reactivity.* HIV-1 antigens gp120<sub>AE.A244</sub> and gp120<sub>M,ConS</sub> were used to test gp120-reactive mAbs; AE.A244 V1V2 tags (WT and K169N) were used to test V2 peptide-reactive antibodies. Surface plasmon resonance binding assays were performed on a BIAcore 4000 (BIAcore Inc.) as described (12).

*ADCC assay.* ADCC activity mediated by plasma against CEM.NKR<sub>CCR5</sub> cells coated with recombinant gp120<sub>AE.92TH023</sub>, gp120<sub>AE.A244</sub>, and gp120<sub>B,MN</sub> was determined using the ADCC-GTL assay as described (41, 42). Cryopreserved human PBMCs from an HIV-1-seronegative donor with the heterozygous 158F/V

genotype for Fc $\gamma$  receptor IIIa were used as the source of effector cells. CD4<sup>+</sup> T cells were activated and infected with AE.CM235 as described (43), and binding to AE.CM235-infected target cells was determined by indirect surface immunofluorescence analysis as described (44).

**Statistics.** Four-parameter logistic regression and determination of the half maximal binding concentration (EC50) of mAbs in ELISA was performed using the *drc* package in R (45). Other statistical tests were performed in SAS v9.4; the test is noted where *P* values are shown. A *P* value of less than 0.05 was considered significant.

**Study approval.** All RMs were housed at the New England Primate Research Center, Southborough, Massachusetts, USA and treated in accordance with the regulation of Association for Assessment and Accreditation of Laboratory Animals with the approval of the Animal Care and Use Committees of the NIH and Harvard Medical School.

### Author contributions

BFH and MAM conceived of and designed the study. KL, HXL, BFH, and MAM wrote and edited the paper. KL, HXL, SSan, NLL, JT, DF, FS, CL, JK, SN, PP, SRN, NLM, JHK, GDT, BFH, and MAM designed individual experiments. CMB, LLS, RMS, and SS performed the animal study. KL, MAM, RZ, DE, TCG, LCA, AAA, TAV, DJM, JFW, JPr, AF, GH, ED, and SA isolated mAbs by memory B cell sorting. KL, DE, RP, KEL, CS, JPe, NLY, JPo, RWE, GF, DCM, GDT, BFH, and HXL performed assays on plasma/serum/mucosa and mAbs. KL, HXL, RZ, DE, KW, SSaw, AW, JPo, SS, SMA, NAV, GF, DCM, GDT, BFH, and MAM analyzed data.

### Acknowledgments

Support for this work was provided by a Collaboration for AIDS Vaccine Discovery grant to BFH from the Bill and Melinda Gates Foundation, by the Center For HIV/AIDS Vaccine Immunology (CHAVI; grant U19 AI067854), and by the Center For HIV/AIDS Vaccine Immunology-Immunogen Discovery grant (CHAVI-ID; grant UM1 AI100645). This study was further supported by CAVD funding for the CTVIMC, grant number OPP1032325; and by the Duke University Center for AIDS Research Flow Cytometry and Virology cores (CFAR; P30-AI-64518).

We thank R. Glenn Overman for expert technical support for mucosal sample processing.

Address correspondence to: M. Anthony Moody or Barton F. Haynes, Duke Human Vaccine Institute, Box 103020 DUMC, Durham, North Carolina 27710, USA. Phone: 919.668.2551 (M.A. Moody); 919.684.5279 (B.F. Haynes); E-mail: moody007@mc.duke.edu (M.A. Moody); hayne002@mc.duke.edu (B.F. Haynes).

1. Robb ML, et al. Risk behaviour and time as covariates for efficacy of the HIV vaccine regimen ALVAC-HIV (vCP1521) and AIDSVAX B/E: a post-hoc analysis of the Thai phase 3 efficacy trial RV 144. *Lancet Infect Dis.* 2012;12(7):531–537.
2. Rerks-Ngarm S, et al. Vaccination with ALVAC and AIDSVAX to prevent HIV-1 infection in Thailand. *N Engl J Med.* 2009;361(23):2209–2220.
3. Haynes BF, et al. Immune-correlates analysis of an HIV-1 vaccine efficacy trial. *N Engl J Med.* 2012;366(14):1275–1286.
4. Tomaras GD, et al. Vaccine-induced plasma IgA specific for the C1 region of the HIV-1 envelope blocks binding and effector function of IgG. *Proc Natl Acad Sci U S A.* 2013;110(22):9019–9024.
5. Gottardo R, et al. Plasma IgG to linear epitopes in the V2 and V3 regions of HIV-1 gp120 correlate with a reduced risk of infection in the RV144 vaccine efficacy trial. *PLoS One.* 2013;8(9):e75665.
6. Zolla-Pazner S, et al. Vaccine-induced IgG antibodies to V1V2 regions of multiple HIV-1 subtypes correlate with decreased risk of HIV-1 infection. *PLoS One.* 2014;9(2):e87572.
7. Yates NL, et al. Vaccine-induced Env V1-V2 IgG3 correlates with lower HIV-1 infection risk and declines soon after vaccination. *Sci Transl Med.* 2014;6(228):228ra39.
8. Chung AW, et al. Polyfunctional Fc-effector profiles mediated by IgG subclass selection distinguish RV144 and VAX003 vaccines. *Sci Transl Med.* 2014;6(228):228ra38.
9. Tay MZ, et al. Antibody-mediated internalization of infectious HIV-1 virions differs among antibody isotypes and subclasses. *PLoS Pathog.* 2016;12(8):e1005817.
10. Rolland M, et al. Increased HIV-1 vaccine efficacy against viruses with genetic signatures in Env V2. *Nature.* 2012;490(7420):417–420.
11. Liao HX, et al. Vaccine induction of antibodies against a structurally heterogeneous site of immune pressure within HIV-1 envelope protein variable regions 1 and 2. *Immunity.* 2013;38(1):176–186.
12. Wiehe K, et al. Antibody light-chain-restricted recognition of the site of immune pressure in the RV144 HIV-1 vaccine trial is

- phylogenetically conserved. *Immunity*. 2014;41(6):909–918.
13. Tomaras GD, Haynes BF. Advancing toward HIV-1 vaccine efficacy through the intersections of immune correlates. *Vaccines (Basel)*. 2014;2(1):15–35.
  14. Corey L, Gilbert PB, Tomaras GD, Haynes BF, Pantaleo G, Fauci AS. Immune correlates of vaccine protection against HIV-1 acquisition. *Sci Transl Med*. 2015;7(310):310rv7.
  15. Chung AW, et al. Dissecting polyclonal vaccine-induced humoral immunity against HIV using systems serology. *Cell*. 2015;163(4):988–998.
  16. Pollara J, et al. HIV-1 vaccine-induced C1 and V2 Env-specific antibodies synergize for increased antiviral activities. *J Virol*. 2014;88(14):7715–7726.
  17. Bonsignori M, et al. Antibody-dependent cellular cytotoxicity-mediating antibodies from an HIV-1 vaccine efficacy trial target multiple epitopes and preferentially use the VH1 gene family. *J Virol*. 2012;86(21):11521–11532.
  18. Bonsignori M, et al. Analysis of a clonal lineage of HIV-1 envelope V2/V3 conformational epitope-specific broadly neutralizing antibodies and their inferred unmutated common ancestors. *J Virol*. 2011;85(19):9998–10009.
  19. Montefiori DC, et al. Magnitude and breadth of the neutralizing antibody response in the RV144 and Vax003 HIV-1 vaccine efficacy trials. *J Infect Dis*. 2012;206(3):431–441.
  20. Kepler TB, et al. Reconstructing a B-cell clonal lineage. II. Mutation, selection, and affinity maturation. *Front Immunol*. 2014;5:170.
  21. Moody MA, et al. HIV-1 gp120 vaccine induces affinity maturation in both new and persistent antibody clonal lineages. *J Virol*. 2012;86(14):7496–7507.
  22. Moody MA, et al. H3N2 influenza infection elicits more cross-reactive and less clonally expanded anti-hemagglutinin antibodies than influenza vaccination. *PLoS One*. 2011;6(10):e25797.
  23. Pancera M, et al. Crystal structure of PG16 and chimeric dissection with somatically related PG9: structure-function analysis of two quaternary-specific antibodies that effectively neutralize HIV-1. *J Virol*. 2010;84(16):8098–8110.
  24. Zwick MB, et al. The long third complementarity-determining region of the heavy chain is important in the activity of the broadly neutralizing anti-human immunodeficiency virus type 1 antibody 2F5. *J Virol*. 2004;78(6):3155–3161.
  25. Ofek G, et al. Structure and mechanistic analysis of the anti-human immunodeficiency virus type 1 antibody 2F5 in complex with its gp41 epitope. *J Virol*. 2004;78(19):10724–10737.
  26. Alam SM, et al. The role of antibody polyspecificity and lipid reactivity in binding of broadly neutralizing anti-HIV-1 envelope human monoclonal antibodies 2F5 and 4E10 to glycoprotein 41 membrane proximal envelope epitopes. *J Immunol*. 2007;178(7):4424–4435.
  27. McLellan JS, et al. Structure of HIV-1 gp120 V1/V2 domain with broadly neutralizing antibody PG9. *Nature*. 2011;480(7377):336–343.
  28. Trama AM, et al. HIV-1 envelope gp41 antibodies can originate from terminal ileum B cells that share cross-reactivity with commensal bacteria. *Cell Host Microbe*. 2014;16(2):215–226.
  29. Jardine JG, et al. HIV-1 vaccines. Priming a broadly neutralizing antibody response to HIV-1 using a germline-targeting immunogen. *Science*. 2015;349(6244):156–161.
  30. Jardine JG, et al. HIV-1 broadly neutralizing antibody precursor B cells revealed by germline-targeting immunogen. *Science*. 2016;351(6280):1458–1463.
  31. McGuire AT, et al. Specifically modified Env immunogens activate B-cell precursors of broadly neutralizing HIV-1 antibodies in transgenic mice. *Nat Commun*. 2016;7:10618.
  32. Liao HX, et al. High-throughput isolation of immunoglobulin genes from single human B cells and expression as monoclonal antibodies. *J Virol Methods*. 2009;158(1-2):171–179.
  33. Volpe JM, Cowell LG, Kepler TB. SoDA: implementation of a 3D alignment algorithm for inference of antigen receptor recombinations. *Bioinformatics*. 2006;22(4):438–444.
  34. Kepler TB. Reconstructing a B-cell clonal lineage. I. Statistical inference of unobserved ancestors. *F1000Res*. 2013;2:103.
  35. Cloanalyst. Boston University Microbiology Laboratory of Computational Immunology. <http://www.bu.edu/computationalimmunology/research/software/>. Accessed November 2, 2016.
  36. Alam SM, et al. Human immunodeficiency virus type 1 gp41 antibodies that mask membrane proximal region epitopes: antibody binding kinetics, induction, and potential for regulation in acute infection. *J Virol*. 2008;82(1):115–125.
  37. Moore JP, et al. Exploration of antigenic variation in gp120 from clades A through F of human immunodeficiency virus type 1 by using monoclonal antibodies. *J Virol*. 1994;68(12):8350–8364.
  38. Gray ES, et al. Antibody specificities associated with neutralization breadth in plasma from human immunodeficiency virus type 1 subtype C-infected blood donors. *J Virol*. 2009;83(17):8925–8937.
  39. Yates NL, et al. HIV-1 gp41 envelope IgA is frequently elicited after transmission but has an initial short response half-life. *Mucosal Immunol*. 2013;6(4):692–703.
  40. Sarzotti-Kelsoe M, et al. Optimization and validation of the TZM-bl assay for standardized assessments of neutralizing antibodies against HIV-1. *J Immunol Methods*. 2014;409:131–146.
  41. Trkola A, Matthews J, Gordon C, Ketas T, Moore JP. A cell line-based neutralization assay for primary human immunodeficiency virus type 1 isolates that use either the CCR5 or the CXCR4 coreceptor. *J Virol*. 1999;73(11):8966–8974.
  42. Pollara J, et al. High-throughput quantitative analysis of HIV-1 and SIV-specific ADCC-mediating antibody responses. *Cytometry A*. 2011;79(8):603–612.
  43. Ferrari G, et al. An HIV-1 gp120 envelope human monoclonal antibody that recognizes a C1 conformational epitope mediates potent antibody-dependent cellular cytotoxicity (ADCC) activity and defines a common ADCC epitope in human HIV-1 serum. *J Virol*. 2011;85(14):7029–7036.
  44. Nelson CS, et al. Combined HIV-1 envelope systemic and mucosal immunization of lactating rhesus monkeys induces a robust immunoglobulin A isotype B cell response in breast milk. *J Virol*. 2016;90(10):4951–4965.
  45. Ritz C, Streibig JC. Bioassay analysis using R. *J Stat Softw*. 2005;15(5):1–22.